Eur. J. Mech. B/Fluids, **17**, n° 6, 847-873, 1998

Experiments on localized disturbances in a flat plate boundary layer. Part 2. Interaction between localized disturbances and TS-waves

A. A. BAKCHINOV ([1]), ([2]) *, K. J. A. WESTIN ([1]) **, V. V. KOZLOV ([2]) and P. H. ALFREDSSON ([1])

ABSTRACT. – Previous studies on boundary layer transition at moderate levels of free stream turbulence (FST) have shown that the transition process can be promoted by the introduction of Tollmien-Schlichting (TS) waves. In the present work the interaction between localized boundary layer disturbances and controlled TS-waves is studied experimentally. The localized disturbances are generated either from a controlled free stream perturbation, or by means of suction or injection through a slot in the flat plate surface. Both methods result in boundary layer disturbances dominated by elongated streamwise streaks of high and low velocity in the streamwise component. A strong interaction is observed preferably for high frequency TS-waves, which are damped when generated separately, and the interaction starts as a local amplification of a wide band of low-frequency oblique waves. The later stages of the transition process can be identified as a non-linear interaction between the oblique structures, leading to regeneration of new and stronger streamwise streaks. © Elsevier, Paris.

Keywords. – Boundary-layer, streaky-structures, transition.

1. Introduction

A laminar boundary layer subjected to rather high levels of free stream turbulence (FST) is dominated by low-frequency fluctuations with large amplitudes in the streamwise velocity component (u). Studies on receptivity to FST has shown that a major contribution to the low-frequency fluctuations originates from non-stationary elongated structures (streaks) with alternatingly high and low streamwise velocity. The general characteristics of these disturbances are discussed in Westin *et al.* (1998) and Westin *et al.* (1994), in which references to related work can be found.

Since the streamwise fluctuations (u_{rms}) can grow to values of the order of 10% of the free stream velocity (U_0) before transition starts, it is a common opinion that TS-waves play a minor or negligible role in this highly disturbed "pseudo-laminar" boundary layer. However, this point of view may partly be biased by the difficulty to detect TS-waves in a boundary layer subjected to FST. In experiments with controlled periodic TS-waves non-linear behaviour can be observed at amplitudes of the order of 1%, and in experiments with more random excitation non-linear events are found at even smaller wave amplitudes (c.f. Shaikh and Gaster 1995). It can therefore be expected that also small amplitude TS-waves can be of importance in a boundary layer disturbed by moderate levels of FST. By introducing TS-waves with a vibrating ribbon, Grek *et al.* (1987, 1990) showed that TS-waves can exist and amplify in a boundary layer subjected to FST-levels of 1-2% of U_0, and that they also affect transition. The same results were obtained in a later experiment by Boiko *et al.* (1994) at a free stream turbulence level of 1.5%. A strong influence of the TS-wave amplitude on the transition onset was found, with a dramatic increase in the number of turbulent spots for higher forcing amplitudes. The non-linear behaviour was initially observed as an amplification of lower frequencies within the unstable frequency band for TS-waves.

* Presently at Chalmers University of Technology, Thermo- and Fluid Dynamics, S-412 96 Göteborg, Sweden.
** Presently at Vattenfall Utveckling AB, S-81426 Älvkarleby, Sweden.
([1]) Dept. Mechanics, Royal Institute of Technology, S-10044 Stockholm, Sweden.
([2]) Institute of Theoretical and Applied Mechanics, Russian Academy of Sciences, Siberian Branch, 630090 Novosibirsk, Russia.

0997-7546/98/06/© Elsevier, Paris

The presence of large amplitude streaky structures in a boundary layer subjected to FST suggests that it can be meaningful to study the interaction between streamwise streaks and TS-waves. This type of model experiments has advantages, since the use of controlled disturbances provides the possibility for ensemble averaging with well-determined phase relations between different disturbances. Interaction between stationary streamwise streaks and periodic TS-waves have been studied by Bakchinov *et al.* (1995a). Large-amplitude spanwise periodic disturbances were generated by means of surface roughnesses, with a disturbance amplitude in the streamwise component of about 35% peak-to-peak. Two different modes were observed: one low-frequency disturbance similar to TS-waves in a two-dimensional (2D) boundary layer, and a high-frequency mode associated with the spanwise gradients in the mean velocity. The latter seemed to be of a local inviscid type, and the authors point out the similarities with the meandering (sinuous) type of secondary instability observed in Görtler flow.

A similar study of a spanwise modulated flat plate boundary layer was carried out by Kachanov and Tararykin (1987). They introduced stationary disturbances by means of suction and blowing through streamwise oriented slits in the plate. The disturbance amplitude was smaller than in the study by Bakchinov *et al.* (1995a), and the simultaneous introduction of small amplitude TS-waves did not result in any dramatic changes. It was shown, however, that the amplitude growth of the 2D component of the introduced TS-wave was smaller in the spanwise modulated boundary layer than in an undisturbed Blasius flow.

Model experiments of the interaction between forced TS-waves and controlled localized disturbances were conducted by Grek *et al.* (1991). The latter disturbances were denoted as "boundary layer puffs", and exhibited characteristics rather different from TS-wave packets. The disturbances showed only a small lateral spreading, and propagated with velocity higher than that of the most unstable TS-waves. Many of the characteristics are similar to the disturbance studied in Westin *et al.* (1998). Grek *et al.* (1991) observed that although the localized disturbance and the TS-wave were damped when generated separately, a simultaneous generation resulted in a strong interaction. Due to the interaction a strong wave-packet appeared, which subsequently developed into a turbulent spot.

The number of experimental studies on interaction between longitudinal streaky structures and TS-waves are rather limited. Considering theoretical and numerical studies, most of them are focussed on streamwise vortices (Görtler and cross-flow vortices) and their interaction with TS-waves. For instance, Malik and Hussaini (1990) have made Direct Numerical Simulations on Görtler vortices combined with 2D and 3D TS-waves, using the parallel-flow approximation. It was shown that non-linear interactions occurred for relatively large amplitudes of the vortices (initial streamwise disturbance amplitude 10% of U_0). If the Görtler vortices are identified as the $(0, \beta)$ modes, the strongest growth was observed for $(0, 2\beta)$, and in the case of a 2D TS-wave $(\alpha, 0)$ non-linear interactions caused a growth in the (α, β) mode as well. Streaks observed at high levels of FST are believed to contain only weak streamwise vortical motions, in contrast to large amplitude Görtler vortices. Thus, the interaction between streaks and TS-waves may be different in the two cases. However, Bottaro and Klingmann (1996) considered secondary instabilities of Görtler vortices, and found that secondary instabilities associated with the spanwise gradients were almost unaffected whether the cross-stream velocity components were included in the calculations or not.

Meitz (1996) carried out Direct Numerical Simulations in which streamwise vortices were introduced in the free stream by means of low-frequency volume forces. The free stream disturbances forced low- and high velocity streaks inside the boundary layer, referred to as Klebanoff-modes. Meitz also studied the interaction between streaks and TS-waves, and found the amplitude growth of the waves to vary in the spanwise direction due to local stabilization or destabilization of the mean flow by the streaks. In the low-velocity regions the TS-wave evolved into 3D wave packets, and transition was obtained for high enough forcing amplitudes of the TS-wave. The observed transition mechanisms were associated with a fundamental type (K-type) of transition, without any indications of subharmonic resonance.

The present paper is based on the ideas of Grek *et al.* (1991), and contains two separate measurements with slightly different methods of disturbance generation. In the first measurement, which in the following will be denoted as experiment A, a localized free stream disturbance was introduced upstream of the leading edge. The boundary layer receptivity and the transformation into a boundary layer disturbance is extensively discussed in part 1 of the present study (Westin *et al.* 1997). Some preliminary results on the interaction between the localized boundary layer disturbance and TS-waves have also been reported in Bakchinov *et al.* (1995b). In the second experiment (experiment B), a localized disturbance was introduced through a small slit in the plate. TS-waves were introduced further downstream, and the interaction between the localized disturbance and the periodic wave was studied.

2. Experimental set-up

The experiments were carried out in the MTL-wind tunnel at the Royal Institute of Technology, Stockholm, using a 1.2×4.22 m^2 flat plate with a 2 m long working part. The leading edge has an asymmetric shape which was specially designed to minimize the non-zero pressure gradient region close to the leading edge. The plate and leading edge configuration is extensively described in Westin *et al.* (1994), but the presently used traversing mechanism is slightly modified. The plate is equipped with a trailing edge flap for adjustment of the stagnation line at the leading edge. In experiment B a fine-meshed screen had to be installed at the rear part of the plate in order to compensate for the blockage below the plate due to the equipment for the disturbance generation.

The coordinate system has its origin at the leading edge, where the streamwise, wall-normal and spanwise directions are denoted x, y and z respectively, and the corresponding velocity components are u, v and w. The free stream velocity (U_0) was 6.6 m/s in experiment A and 6.75 m/s in experiment B. The measurements were carried out with hot-wire anemometry, and a single wire probe of length 0.5 mm and wire diameter 2.5 μm was used in most cases. In experiment A two computers were used: one for data acquisition and one for controlling the servo motors for the traversing mechanism, and the disturbances were generated by a separate function generator. In experiment B the same computer was used for all purposes (traversing the probe, disturbance generation and data acquisition).

2.1. Disturbance generation: Experiment A

The localized disturbance was generated by a loudspeaker connected to a small pipe (inner diameter 1 mm), with its tip positioned 12 mm upstream of the leading edge (*see* figure 1). The y-position of the pipe was carefully adjusted to obtain a disturbance with a trajectory that reached the working side of the plate, and at the same time to avoid any influence from the wake of the pipe. To generate the disturbance, a function generator was connected to a pulse generator, giving a short duration pulse at a frequency typically $f_0/64$ (f_0 is the frequency of the function generator). A second disturbance was obtained from an additional loudspeaker connected to a 35 mm long and 0.6 mm wide slit in the plate, positioned at $x = 95$ mm. The loudspeaker was forced by the signal from the function generator (amplified by an audio amplifier), resulting in a periodic TS-wave with frequency f_0. The same function generator was used both for the TS-wave generation and the triggering of the localized disturbance, giving a definite phase relation between the two disturbances.

2.2. Disturbance generation: Experiment B

In experiment B the localized disturbance was obtained from a loudspeaker connected to the spanwise slit positioned at $x = 95$ mm, but the length of the slit was reduced to approximately 3 mm. In earlier experiments (Bakchinov *et al.* 1997) it has been observed that the generation of streaks is more efficient if the spanwise

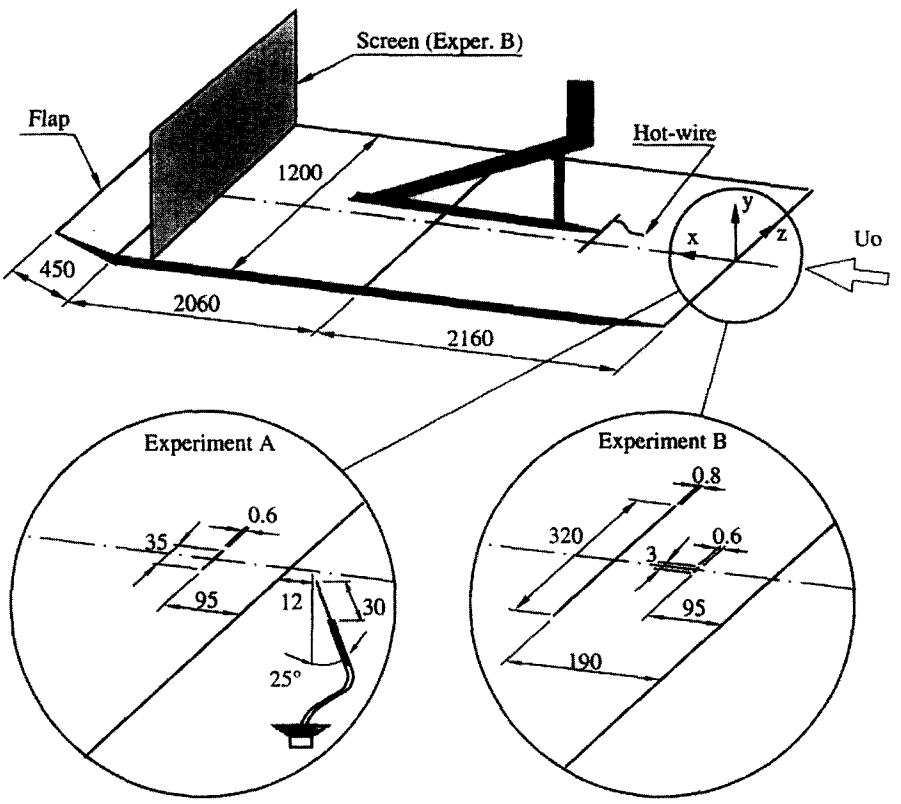

Fig. 1. – Outline of experimental set-up. Dimensions in mm.

extent of the slit is not too small in comparison with the local boundary layer thickness (δ_{99}). In the present case the length was chosen to be of the order of the boundary layer thickness at the position of the source. The output signal was generated by an analog output board, and amplified with a DC-amplifier. Special care was taken to obtain a boundary layer disturbance with energy centred around a zero-streamwise wavenumber (the aim was to generate a long streaky structure similar to the one obtained in experiment A). The output disturbance had a shape close to a square wave but with slightly inclined flanks (linear ramps of 10 ms), and the period time was 0.75 s. This resulted in two separate disturbances, i.e. injection of air at the upward going flank, and suction of air through the slit at the downward going flank.

The periodic TS-wave was generated by a 320 mm long slit positioned at $x = 190$ mm, which in the present experiment corresponds to a Reynolds number R of 500. (R is the Reynolds number based on the displacement thickness in a Blasius boundary layer, i.e. $R = 1.72\sqrt{U_0 x/\nu}$ in which ν is the kinematic viscosity. When the experimentally determined displacement thickness (δ^*) is used to define the Reynolds number, this is denoted as $Re_{\delta^*} = U_0\delta^*/\nu$.) The equipment for generation of TS-waves is the same as used by Elofsson and Alfredsson (1997), which consists of a number of pipes connected to the lower side of the plate and distributed in the spanwise direction (the set-up was adopted from Bake *et al.* (1995) and Gaponenko and Kachanov (1994)). The orifices of the pipes are flattened before they enter into a cavity inside the plate, which in turn is connected to the slit. In the present experiment two loudspeakers were used, each of them connected to 10 pipes. Both loudspeakers were forced with the same frequency, and the signals were generated by the analog output board and amplified with an audio amplifier.

2.3. Measurement technique and data processing

Two or three separate measurements were carried out at each position in space: Generation of (1) the localized disturbance, (2) the periodic wave and (3) simultaneous generation of the localized disturbance and the wave. The different sets of data were collected sequentially before the probe was moved to the next position, to avoid any influence from small inaccuracies in the positioning of the traversing mechanism.

In the present paper the structure of the disturbance is presented as contour plots showing (y,t)- or (z,t)-planes, i.e. measured either in the wall-normal or spanwise direction and with time (t) as the second variable. The distributions show the streamwise velocity disturbance, which is defined as the deviation from the local mean velocity in the undisturbed flow.

Since the study is focussed on the behaviour of the deterministic part of the signal, ensemble averaging was carried out at each measurement point. The chosen number of averages varied slightly depending on the characteristics of the signal, but a typical number of averaged realizations was 50 in experiment A and 30 in experiment B (the repeatability was better when the localized disturbance was generated from the slit).

The measured (z,t)-distributions were decomposed by temporal and spatial Fourier transforms. Usually the spacing between the measurement points was increased far from the centreline, and since the Fourier transform routines require an equidistant distribution, linear interpolation was applied in the spanwise direction. The step size was determined by the spanwise resolution used in the central part of the measurement region. Since the present flow consists of a periodic wave train as well as a localized disturbance, it is not obvious how to normalize the spectra. In the present paper amplitude spectra are used, which means that each spectrum is normalized with the size of the transformed domain. This implies that the energy contribution from the periodic disturbance is independent of the domain size, while the spectral peaks corresponding to the localized disturbance will be reduced when the domain is increased. However, by using a constant size of the transformed time and space domain, the amplitudes in different spectra can be directly compared. In cases where a smaller spanwise measurement region was available, additional zeros were padded. Neither f (=1/T) nor β $(= 1/\lambda_z)$ are normalized, and their units are Hz and m^{-1} respectively (T is the period time, and λ_z denotes the spanwise wavelength).

2.4. Mean flow characteristics

As mentioned in Part 1 of the present paper the mean velocity profiles in the undisturbed flow are close to the Blasius distribution, which can be observed already at $x = 15$ mm. Although the number of measurement points inside the boundary layer is relatively small, the shape factor ($H = \delta^*/\theta$, in which δ^* and θ is the displacement thickness and the momentum loss thickness respectively) differs less than 1.5% from the theoretical value (2.59) for all measured profiles. The short region with non-zero pressure gradient can be ascribed to the shape of the leading edge, and the pressure variation was less than 1% of the dynamic pressure for $x > 20$ mm (c.f. Klingmann *et al.* 1993 for a discussion about leading edge effects and the influence on TS-waves).

3. Results: Experiment A

3.1. The localized boundary layer disturbance

The localized boundary layer disturbance is generated by a short duration free stream perturbation that impinges onto the laminar boundary layer close to the leading edge. The perturbation causes a wall-normal displacement of fluid elements, which together with the mean shear inside the boundary layer results in regions of high and low streamwise velocity. During the downstream development these high- and low-velocity regions are stretched out

in the streamwise direction, forming longitudinal streaky structures with narrow spanwise scales. The dominating spanwise wave length is about two times the boundary layer thickness for the downstream positions, while the streamwise extent is an order of magnitude larger. However, although the perturbation amplitude is high close to the leading edge (peak-to-peak amplitude $u_{pp} \approx 25\%$ at $x = 35$ mm), the amplitude decays downstream and the disturbance finally disappears. The receptivity and evolution of the localized disturbance is extensively described in Part 1 of the present paper (Westin *et al.* 1998).

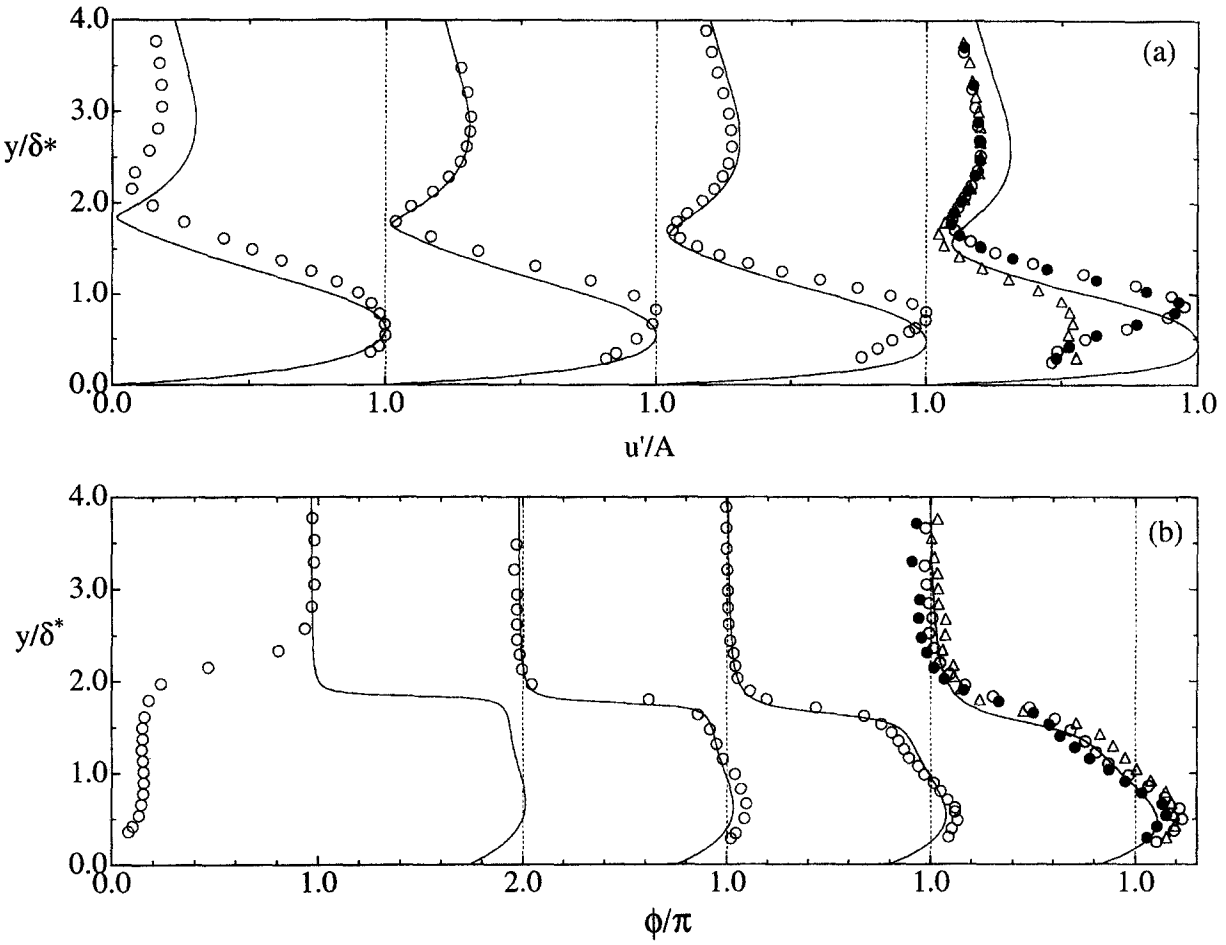

Fig. 2. – Amplitude (a) and phase (b) profiles of the generated TS-wave in experiment A ($F = 455$). The x-positions are from left to right x=100, 125, 160 and 200 mm ($Re_{\delta*}$=370, 405, 460 and 520). Labels: z=0 mm (○); z=-2.75 mm (•); z=5.25 mm (△); Linear PSE-calculations (—). Note that each amplitude profile at the last x-position is normalized to a value of 0.2 at the outer maximum.

3.2. The periodic TS-wave

The objective of the experiment was to study the interaction between the localized disturbance and a periodic TS-wave. The frequency of the wave was chosen to get as large interaction as possible for a constant adjustment of the amplifier. The strongest interaction was observed for frequencies in a band between 180 and 230 Hz, and a frequency (f_0) of 210 Hz was chosen for the present measurements. This corresponds to a non-dimensional frequency ($F = 2\pi f_0 \nu \cdot 10^6/U_0^2$) of 455, which is a highly damped TS-wave in the Blasius boundary layer. The initial amplitude of the wave was large, about 2.5% of U_0 at $x = 100$ mm, but it decayed quickly

downstream to an amplitude of 0.8% at $x = 200$ mm. (The TS-wave amplitude (A) is measured at the inner maximum, and is defined as the rms-value of the spectral component (f_0) obtained after Fourier transformation of the averaged signal).

In figure 2 amplitude and phase profiles for the TS-wave are shown at different downstream positions measured on the centreline ($z = 0$). These are compared with results from a linear PSE-calculation (Parabolized Stability Equations) for a two-dimensional TS-wave. The first position ($x = 100$ mm) corresponds to a distance only 5 mm downstream of the slit, but the profiles have shapes which clearly show the characteristics of a TS-wave.

The profiles measured further downstream show a continuous movement of the location of the inner amplitude maximum towards larger y, which is probably caused by an increased spanwise distortion of the wave fronts. This can be expected, since the spanwise extent of the slit is only 35 mm, and it is also difficult to achieve a uniform injection of air along the slit. Despite a continuous downstream decay of the TS-wave amplitude, spanwise variations of the amplitude could be observed with a tendency towards the formation of peaks and valleys at $x = 200$ mm. This can also be detected in the profiles measured at different spanwise positions in figure 2a, in which $z = 5.25$ mm corresponds to a valley while the other two profiles are closer to an amplitude peak. It should be noticed that the amplitude profiles at $x = 200$ mm are a result of superposition of 2D and 3D waves with frequency f_0. PSE-calculations gave a phase velocity of $0.44U_0$ and a streamwise wavelength of 13.9 mm for a 2D wave with F=455, which is in good agreement with the experimentally determined values.

The high amplitude of the TS-wave and the spanwise distortion which introduces non-zero β in the spectra are not desirable characteristics for the present model experiment, and it clearly makes it difficult to interpret the results from the interaction with the localized disturbance. This was also one of the motivations for extending the study with a new experiment (B). However, the first experiment provides interesting results for later comparisons with experiment B, and some of the more important findings from the study of the interaction are summarized below.

3.3. Interaction between the localized disturbance and the TS-wave

A qualitative impression of the effect of the interaction can be obtained from figure 3, which shows peak-to-peak amplitudes (u_{pp}) of the ensemble averaged disturbances. u_{pp} was determined by making a spanwise traverse approximately at the y-location where the largest perturbation amplitude was observed, whereafter a

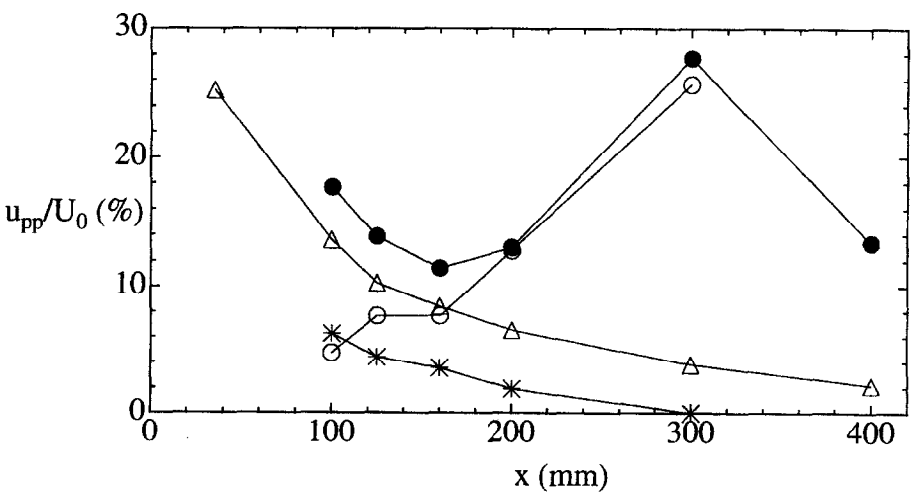

Fig. 3. – Downstream development of the maximum peak-to-peak amplitude of the streamwise disturbance velocity (u_{pp}) in experiment A: localized disturbance (△), TS-wave (*), total disturbance (•), total disturbance with initial disturbances subtracted (o).

few (y,t)-planes were measured in the most interesting regions. As observed in part 1 of the present paper the amplitude of the localized disturbance is decaying downstream, although the initial amplitude is high. Also the TS-wave is continuously damped, despite the large initial amplitude. However, when the two disturbances are generated simultaneously, the total disturbance amplitude is decaying initially, but between $x = 160$ mm and $x = 300$ mm a rapid amplification is observed. Further downstream the evolution of the perturbation becomes more stochastic, and approximately 15% of the generated disturbances continue to grow in amplitude and evolve into turbulent spots. However, most of the disturbances start to decay, thus leading to a lower peak-to-peak value for the averaged disturbance amplitude at the last measurement position. The strong effect of the interaction can also be seen in figures 4a-d, which compare the velocity distribution of the localized disturbance with or without simultaneous generation of TS-waves.

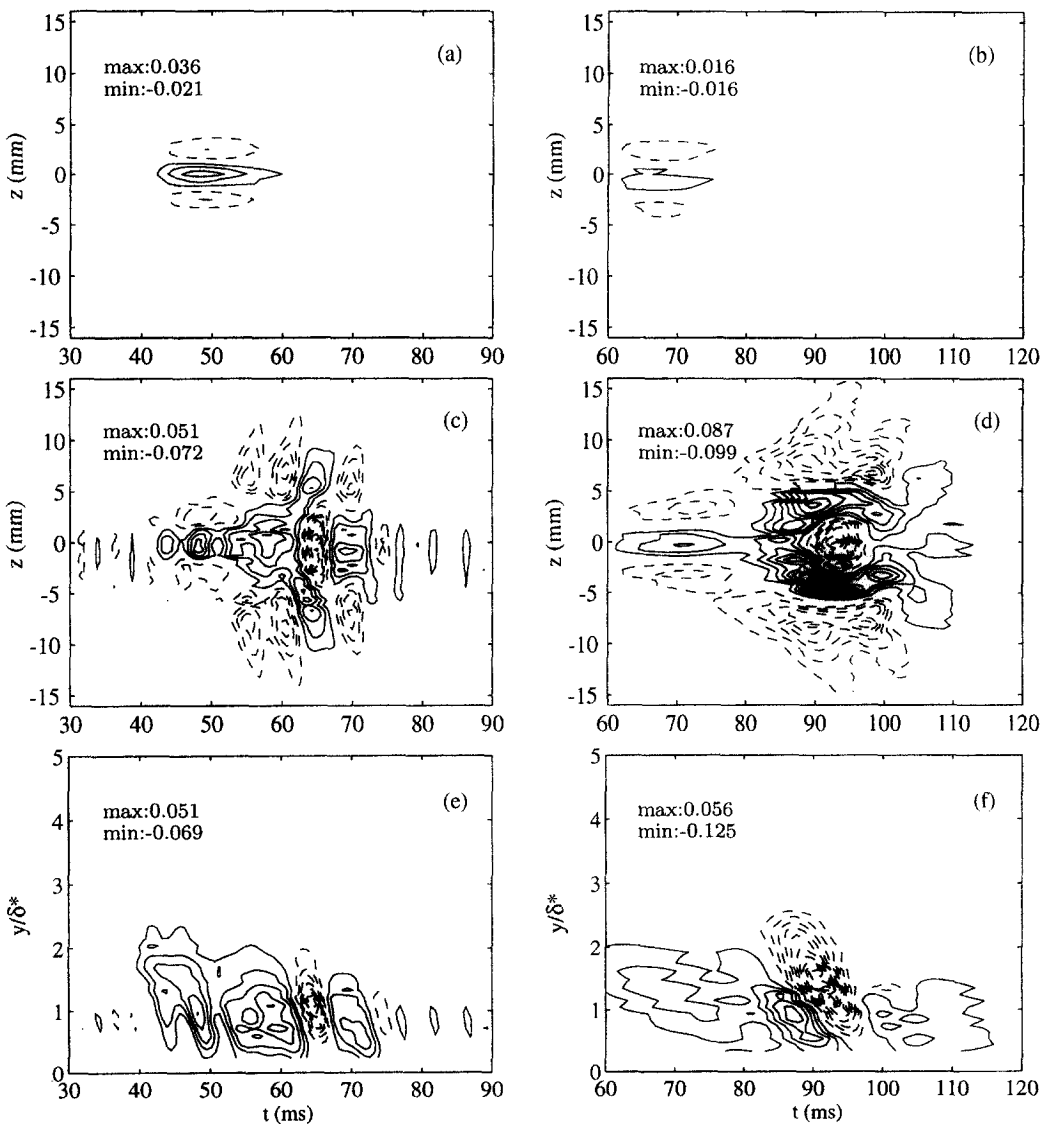

Fig. 4. – Spanwise (a-d) and wall-normal (e,f) distributions of the velocity perturbation in experiment A. (a) and (b) show the localized disturbance, while (c-f) show the result of the interaction (total disturbance). Measurement positions: (a,c) $x = 200$ mm, $y = \delta^*$; (b,d) $x = 300$ mm, $y = 1.2\delta^*$; (e) $x = 200$ mm, $z = 0$; (f) $x = 300$ mm, $z = 0$. Contour spacing: $0.01U_0$.

The first positions where measurements of the interaction between the TS-wave and the localized disturbance were conducted are at $x = 100$ and $x = 125$ mm (not shown). The strongest interaction was observed in both the low and high velocity regions of the localized disturbance close to a y-location corresponding to the TS-wave maximum, but not in the positions of the maximal spanwise shear layers.

In figure 4c, showing the spanwise distribution at $x = 200$ mm, a Λ-shaped structure appear on the centreline. The disturbance has also spread in the spanwise direction with a wave pattern on the flanks. It should be emphasized that the aspect ratio of the figure is misleading, and the structure is more aligned with the flow direction than it appears in the figure. At the consecutive station (figure 4d, $x = 300$ mm), the oblique structure observed at $x = 200$ mm has tilted even more in the mean flow direction, and at positions further downstream new streamwise streaks appear. Figure 4 also shows that the structure generated by the interaction has a lower propagation velocity than the streaks corresponding to the intial localized disturbance.

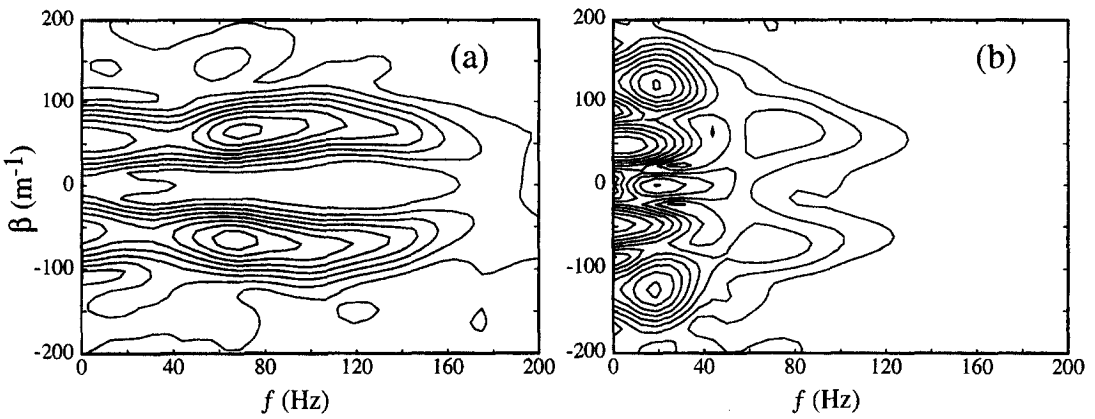

Fig. 5. – (f, β) spectra of the interaction in experiment A. (a) $x = 200$ mm, $y = 0.98\delta^*$; (b) $x = 300$ mm, $y = 1.3\delta^*$. Contour spacing: (a) $0.05U_0$; (b) $0.1U_0$.

The spanwise distributions of the velocity perturbation were Fourier transformed and some of the frequency – spanwise wavenumber (f, β) spectra are shown in figure 5. At $x = 100$ mm and $x = 125$ mm (no spectra are shown), most of the energy was observed in a wide frequency band around the central frequency $f_0 = 210$ Hz and $\beta \approx \pm 200$ m^{-1}, which corresponds to the frequency f_0 of the generated TS-wave and a spanwise wavenumber close to the dominating β of the localized disturbance. This is also the type of interaction that one should expect from these initial disturbances, since non-linearly induced spectral peaks can be obtained from vector addition in the (f, β)-plane.

Further downstream, (figure 5a) the dominating peaks appear at lower frequencies and wavenumbers. At $x = 200$ mm most of the energy is centred around $\beta \approx \pm 60 - 70$ m^{-1} and $f \approx 65$ Hz, although there is energy continuously distributed from $f = 0$ to well above 100 Hz. A rough estimation of the wave angle, based on the spectral peaks at $(f, \beta) \approx (65, \pm 65)$ and assuming a propagation velocity $c = 0.5\,U_0$ for the TS-wave, gives an angle of 73°. This is consistent with the manifested oblique structure in figure 4c, although the wave angle (i.e. the angle between the wave vector and the x-axis) apparently looks smaller since the structure is compressed in the time direction.

In figure 4d it can be observed that the Λ-shaped structure at $x = 200$ mm evolves into a disturbance which is more aligned with the flow direction at the consecutive measurement positions. In the corresponding

spectrum (figure 5b) most of the energy appear around $f \approx 20$ Hz, $\beta \approx \pm 120$. There is also energy concentrated around $\beta \approx 50$ m^{-1} and zero frequency, which can be associated with the negative regions at the flanks of the disturbance in figure 4d. The spectral peaks at $\beta \approx \pm 120$ might be explained as the result of a non-linear interaction between the oblique structures at $x = 200$ mm. If the spectral components $(f_1, \beta_1) \approx (65, \pm 65)$ interact non-linearly, this should result in energy at components $(0, 2\beta_1) = (0, \pm 130)$, i.e. close to the peaks in figure 5b (it should be mentioned that also other modes can gain energy from the suggested non-linear interaction, although they are less likely to be excited).

The interaction between the localized disturbance and the high amplitude TS-wave in experiment A can roughly be divided into three main stages:

(1) non-linear generation of energy in a wide band of frequencies and spanwise wave numbers centred around $(f, \beta) \approx (210, \pm 200)$;
(2) energy growth at lower frequencies and the formation of distinct oblique structures;
(3) non-linear generation of streaky structures.

These observations should be kept in mind while considering the results of experiment B.

4. Results: Experiment B

4.1. The localized disturbances

As mentioned in section 2.2, special care was taken to obtain a localized disturbance with most of the energy centred around a zero streamwise wavenumber. It was also decided to measure both suction and injection through the slit during the same period using the same output voltage to the loudspeaker. This implies that the maximum amplitude is limited by the stronger disturbance obtained for the injection case, and the amplitude and the shape of the loudspeaker-signal were adjusted to obtain as strong disturbance as possible without generating a turbulent spot.

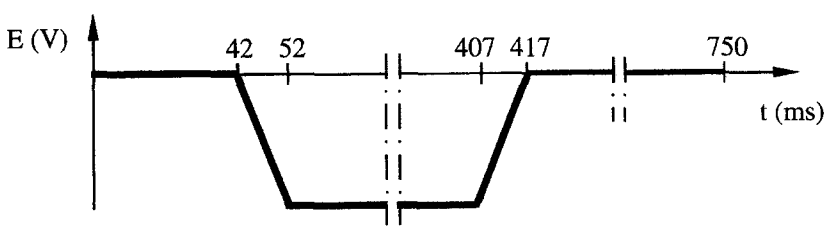

Fig. 6. – Output voltage to the loudspeaker triggering the localized disturbances.

Figure 6 shows the shape of the loudspeaker-signal that was used. The linear ramps are important in order to smooth the disturbance, and a pure square wave results more easily in a turbulent spot. At the first downward going ramp a localized disturbance is triggered due to suction, and, later in the same period, a second disturbance is generated by means of injection at the upward going ramp.

Figures 7 and 8 show the downstream development of the localized disturbance that is obtained for the case of suction and injection respectively. The spanwise distributions are measured at a y-position corresponding to the maximum perturbation amplitude on the centreline. As expected, the peak-to-peak amplitude is smaller in the suction case, and the spanwise scale is larger than in the case of injection. Both disturbances have a long tail on the centreline. The second position (200 mm) is close to the location where the TS-wave is introduced, and

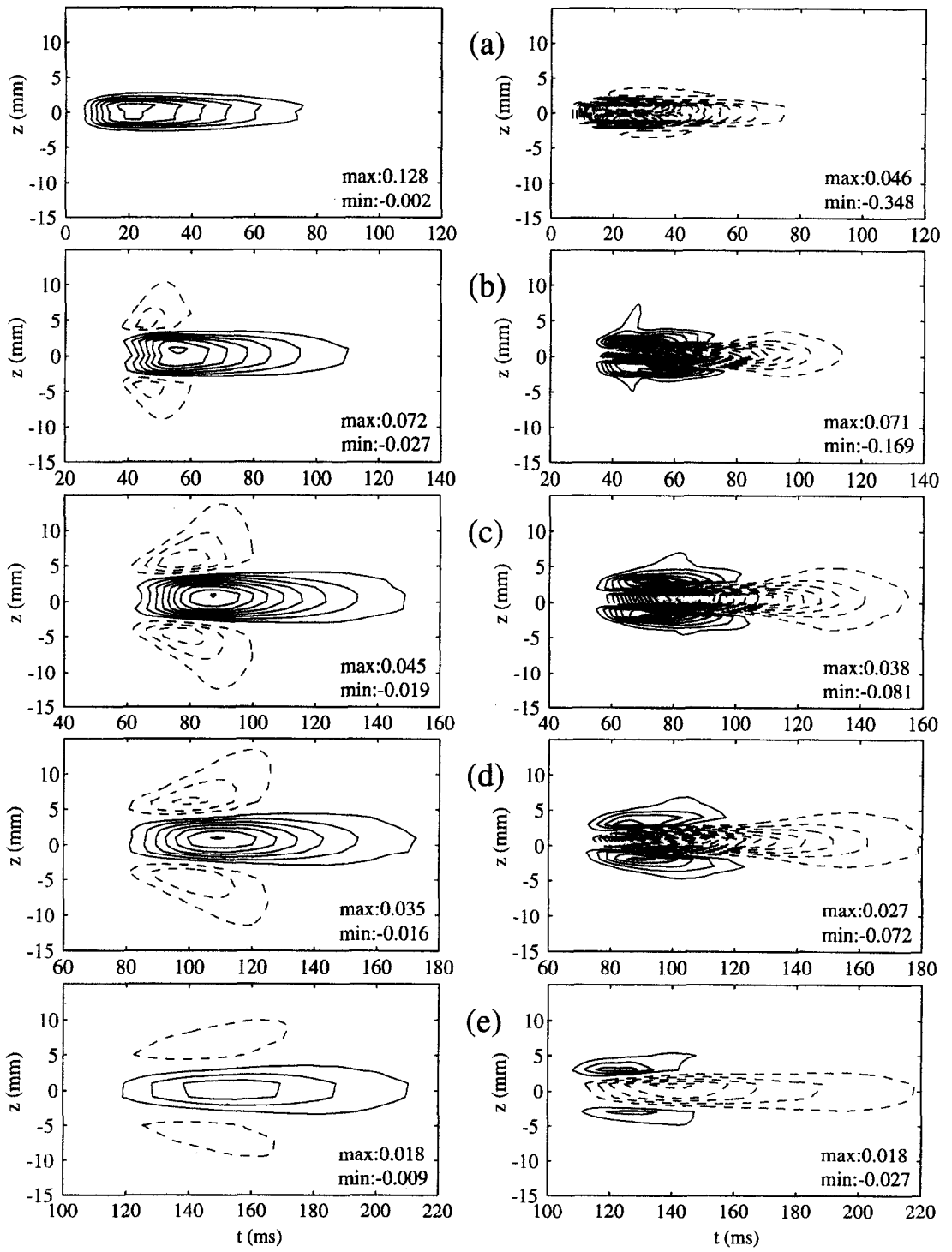

Fig. 7. – Spanwise distributions of the perturbation velocity (u) for the localized disturbances in experiment B. The y-positions correspond to the maximum amplitude on the centreline (suction). The x-positions are from top to bottom x=100, 200, 300, 400 and 600 mm ($Re_{\delta*}$=355, 510, 615, 720 and 880). Contour spacing: (a) $0.02U_0$; (b) $0.01U_0$; (c)-(e) $0.005U_0$. Peak amplitudes are given in each figure. Left and right columns correspond to suction and injection respectively.

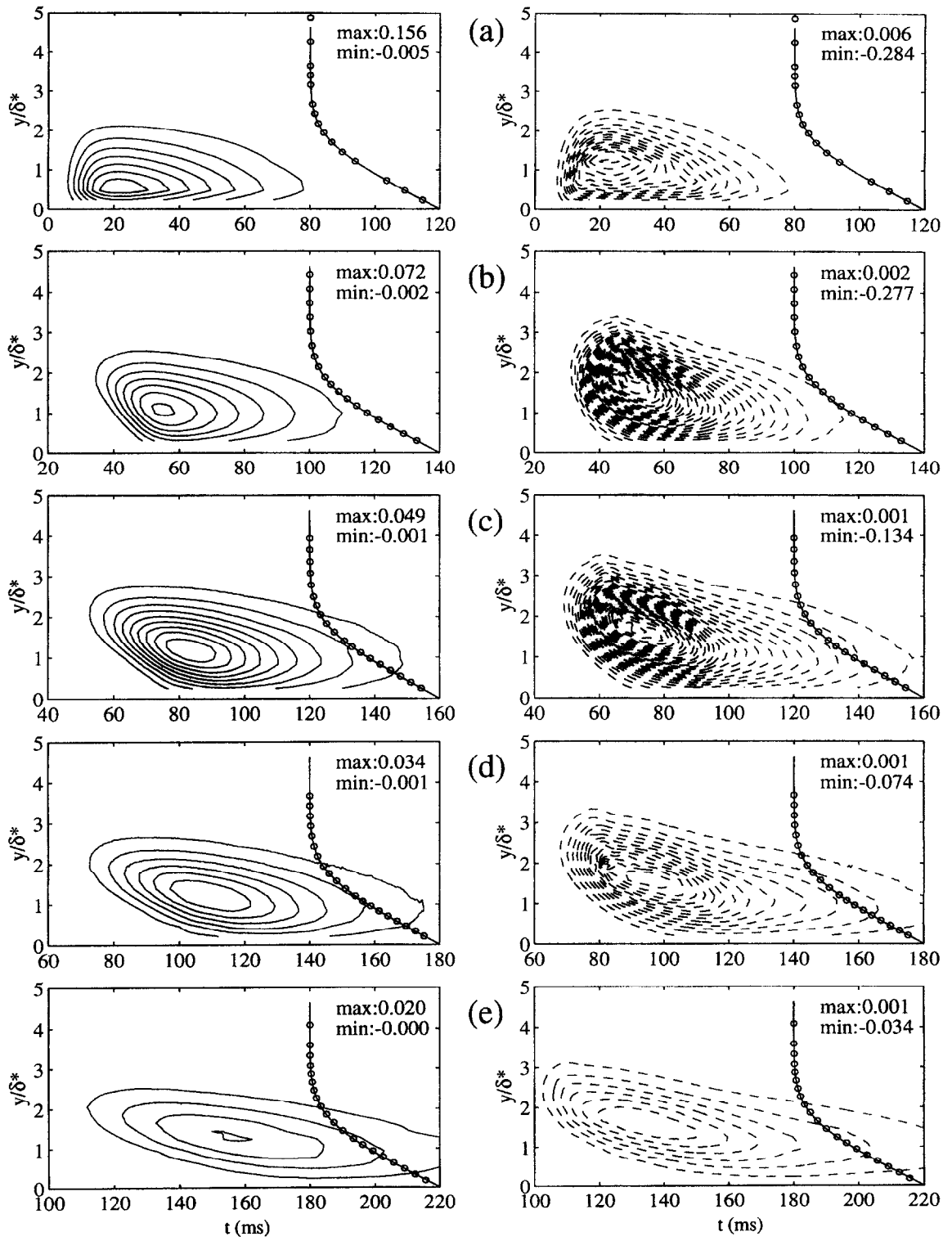

Fig. 8. – Wall-normal distributions of u for the localized disturbances in experiment B measured at $z = 0$. x-positions and contour levels are the same as in the previous figure. Mean velocity profiles measured in the undisturbed flow (o) are also shown together with the Blasius solution. Left and right columns correspond to suction and injection respectively.

the peak-to-peak amplitudes, extracted from the available distributions of u, are approximately 10% and 35% for the two cases respectively. The spanwise gradients possess even larger differences, since the disturbance obtained in the injection case is not only stronger, but also more narrow in the spanwise direction.

One of the aims with experiment B was to generate a localized disturbance similar to the one in experiment A (*see* Westin *et al.* , 1998), with characteristics resembling the streamwise streaks which can be observed at high levels of FST. It seems that the disturbance obtained by suction through the slit is closer to the disturbance in experiment A, with a positive streak on the centreline surrounded by two negative regions. However, the disturbance in experiment B is both wider and longer than the localized disturbance in experiment A at the same Reynolds number. The disturbance structure in the injection case has qualitatively the opposite phase. However, it has a spanwise scale, at least in the front part of the disturbance, which more closely matches the disturbance in experiment A.

The spectra shown in figure 9 are obtained from Fourier transformation of the corresponding velocity distributions in figure 7 at $x = 200$ mm. In the suction case the energy is centred around two peaks at $f = 0$ and $\beta \approx \pm 40$, although the energy is distributed to wavenumbers well above ± 100. At the following two x-positions the dominating β increases to 50, which corresponds to a spanwise wave length of 20 mm. This is larger than one may expect by looking at the contours in figure 7, but can be ascribed to the obliqueness of the negative regions in the front part of the disturbance which gives a smaller β as compared to more streamwise oriented structures. In the case of injection the energy is distributed over a wide range of spanwise wavenumbers. The peaks appear at $\beta \approx \pm 170$, but these are not very distinct and there is a significant energy contribution in the range $\beta \in (-400, 400)$ m^{-1}.

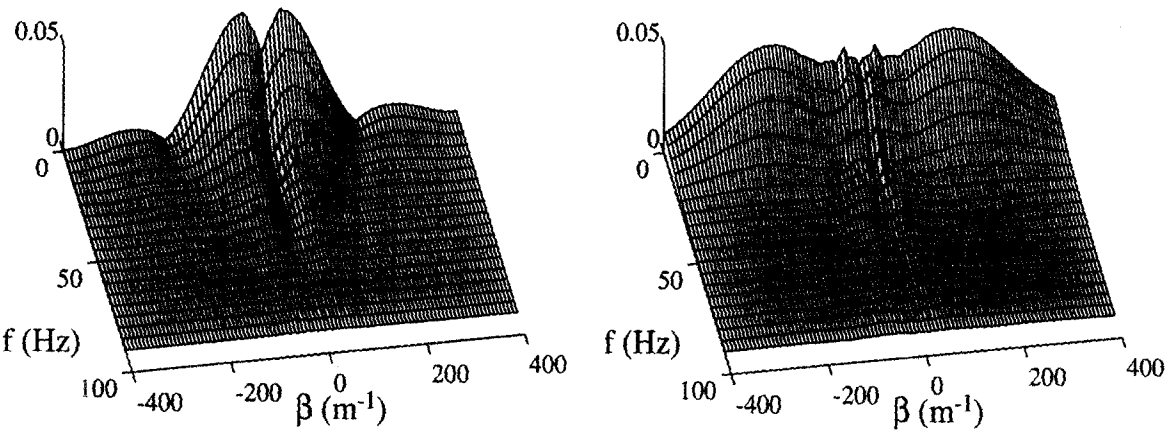

Fig. 9. – Frequency (f) - spanwise wavenumber ($\beta = 1/\lambda_z$) amplitude spectra for the localized disturbance at $x = 200$ mm ($Re_{\delta^*} = 510$). Left and right figure correspond to suction and injection respectively.

The high perturbation velocity in the localized disturbance implies that inflection points may exist, which can have a strong destabilizing effect on TS-waves. Figure 10 displays the second derivative of the instantaneous velocity profile on the centreline, and inflection points exist at some time instants both in the suction case and in the injection case. The former has an inflection point close to the wall, while the dangerous inflection point in the injection case is further from the wall at $x = 200$ mm. (According to the theorem of Fjørtoft the flow is unstable if $U''(U - U_s) < 0$, in which U_s is the velocity at the inflection point and U is the mean velocity somewhere in the flow. In the boundary layer this criterion is fulfilled only when U'' changes from positive to negative sign for increasing y.)

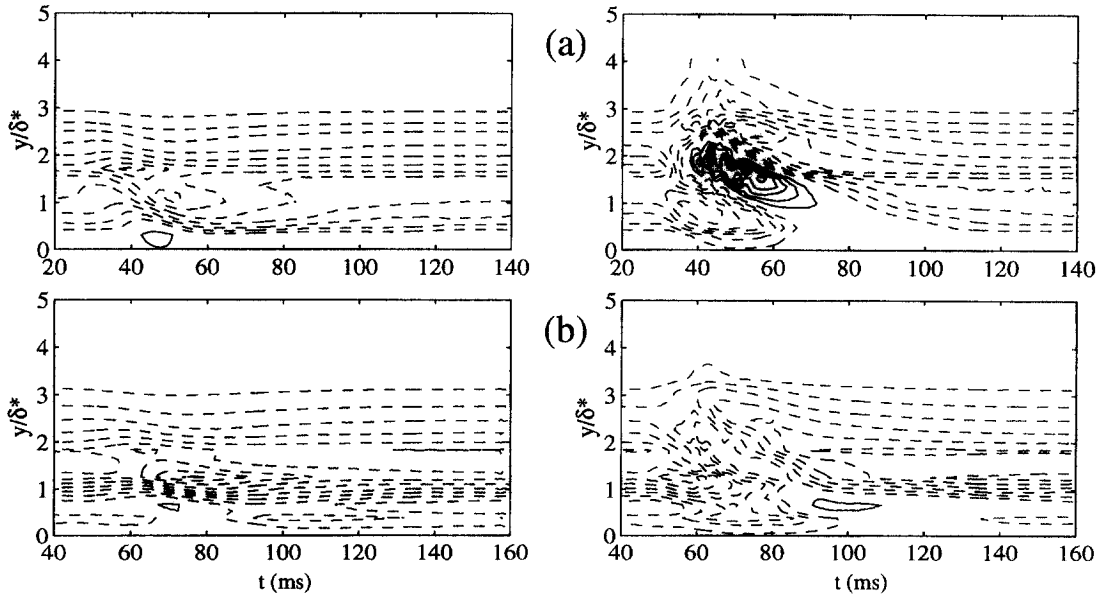

Fig. 10. – Second derivative $(\partial^2 U/\partial y^2)$ of the wall-normal distributions at $z = 0$. (a) $x = 200$ mm; (b) $x = 300$ mm. Left and right columns correspond to suction and injection respectively. Contour spacing: (a) 0.3 and (b) 0.2 ($\times 10^6$ (ms)$^{-1}$).

4.2. The periodic TS-wave

The procedure for determining an appropriate TS-wave frequency was similar to experiment A, i.e. different frequencies were generated with a constant output voltage to the loudspeaker, and the strongest interaction with the localized disturbance was observed in a frequency band $f \in (100, 150)$ Hz. Measurements of the TS-wave amplitude at $x = 250$ mm showed a maximum at $f \approx 130$ Hz, and it was decided to avoid this frequency since it might correspond to a resonance frequency for the slit and the loud-speaker configuration. The generation frequency for the TS-wave (f_0) was therefore set to 120 Hz, which corresponds to $F = 250$ at the present free stream velocity (6.75 m/s). It should be emphasized that the chosen frequency is not necessarily the one which gives the strongest interaction for a specified wave amplitude. To find that "optimal frequency" the output voltages to the loud-speakers have to be adjusted to obtain a constant TS-wave amplitude for each frequency, which was not done in the present study.

Amplitude and phase profiles of the generated TS-wave are shown in figure 11, and the downstream development of the maximum amplitude (measured at the inner maximum of the TS-wave) are shown in figure 12. In both figures the experimental results are compared with linear PSE-calculations, showing satisfactory agreement. The larger deviation at the first measurement position can be ascribed to the short distance downstream of the slit (10 mm), and it can be expected that the wave is still influenced by the disturbance source. The calculated phase velocity is approximately $0.42U_0$, which in the present case gives a streamwise wavelength (λ_x) of 23.6 mm.

A major concern in experiment A was the large amplitude of the TS-wave and the three-dimensional distortion of the wave fronts. The TS-wave amplitude A, i.e. the rms-value of the Fourier component corresponding to f_0, is in experiment B 0.95% of U_0 at $x = 200$ mm. At the last x-position (600 mm) the amplitude is less than 0.01%, which explains why the amplitude and phase-profiles in figure 11 look somewhat distorted. The two-dimensionality of the wave is improved in experiment B due to the wider slit. Since a number of pipes are connected to the slit this might introduce a spanwise periodicity in the TS-wave amplitude. This was checked by Fourier transformation of the signal measured in the spanwise direction, and a small contribution to the

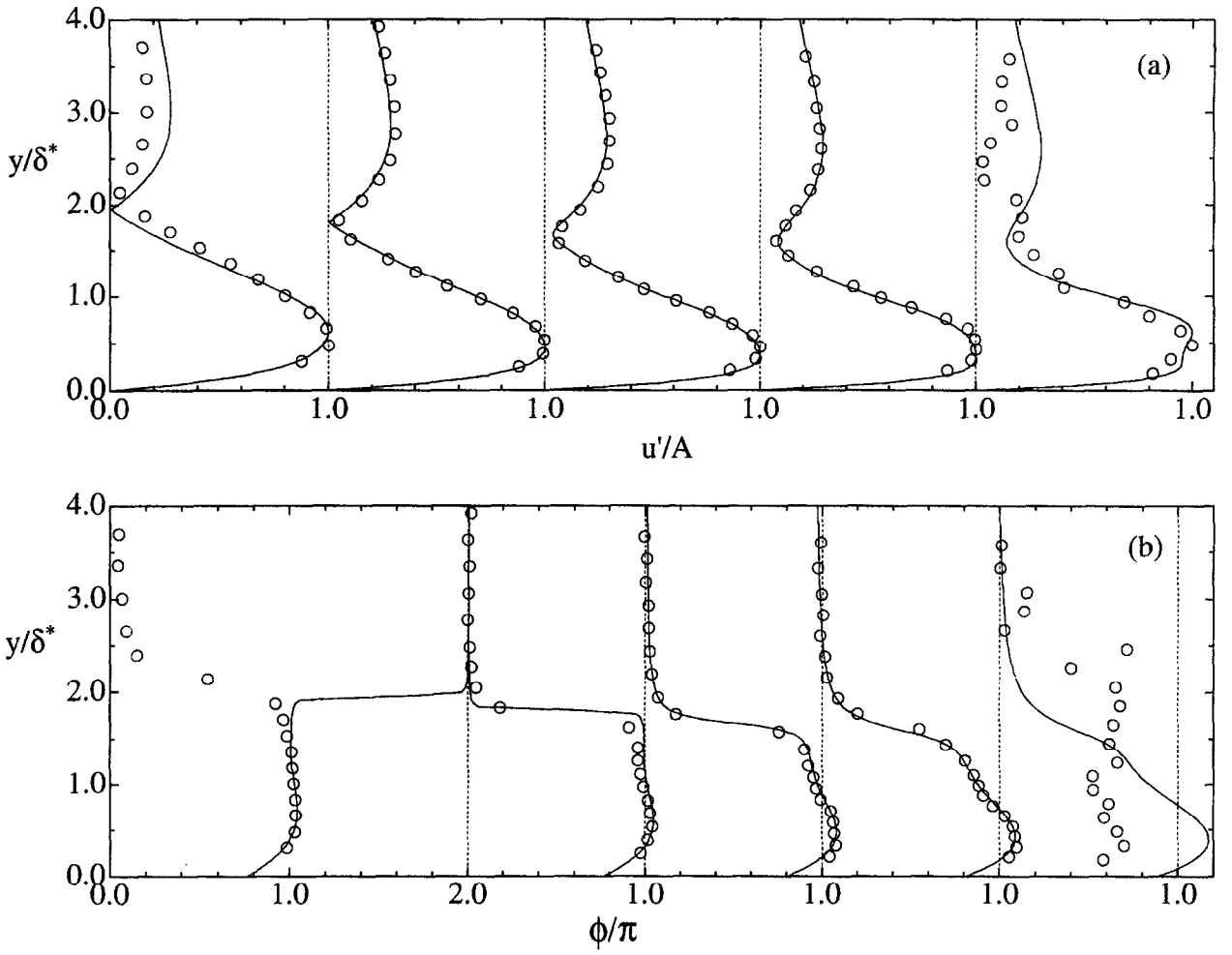

Fig. 11. – Amplitude (a) and phase (b) profiles of the generated TS-wave in experiment B ($F = 250$). The x-positions are from left to right x=200, 300, 400, 500 and 600 mm ($Re_{\delta*}$=510, 615, 720, 800 and 880). Labels: experiment (o); linear PSE-calculation (—).

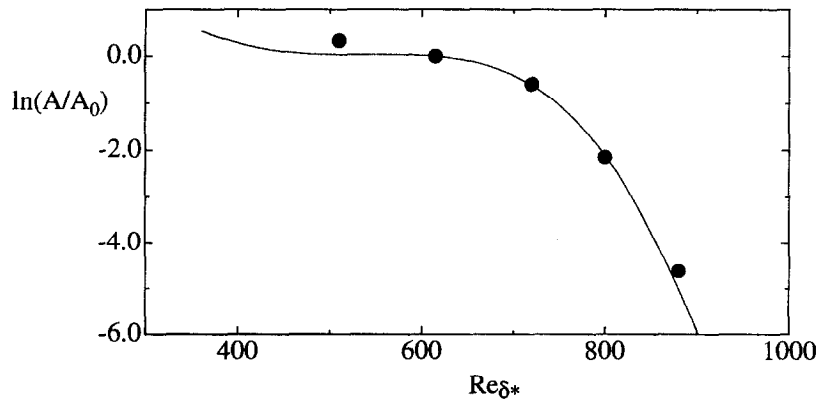

Fig. 12. – Amplitude evolution for $F = 250$ measured at the inner maximum. Experiment (•); linear PSE-calculation (—). Both curves are normalized at $Re_{\delta*} = 615$.

spectra could be observed at $\beta \approx 62$ m^{-1}. This corresponds to the distance between the pipes in use, which was 16 mm. However, the ratio between the energy centred around the 2D component and the energy around $\beta = \pm 62$ m^{-1} was about 500 at $x = 200$ mm, with an increasing ratio downstream. Consequently, it is believed that the introduced TS-wave in experiment B is sufficiently two-dimensional.

It should be noticed that the receptivity of the boundary layer to the TS-waves in both experiments A and B might be somewhat different in the case when the localized disturbances are generated upstream from the TS-wave source. This aspect has not been investigated in detail in the present paper.

4.3. Interaction between the localized disturbances and the TS-wave

Figures 13 and 14 show the downstream development of the total disturbance velocity (u) that is obtained when the TS-wave interacts with the localized disturbances. If we first consider the suction case, it is possible to recognize a similar scenario as in experiment A. The positive region on the centreline starts to deform, and at $x = 400$ mm a strong negative region surrounded by a Λ-shaped structure can be observed. This structure shows clear similarities with the one shown in figure 4c. The negative disturbance on the centreline increases in magnitude, and at the following measurement station the total disturbance has a peak-to-peak amplitude of about 40% of U_0. Finally, at $x = 600$ mm, new streamwise streaks are generated. It should be mentioned that the disturbance did not evolve into a turbulent spot, but the amplitude started to decay further downstream.

Considering the injection case, the interaction looks somewhat different. Initially, the strong localized disturbance is enhanced by the interaction, while the overall shape is maintained. It is also possible to see the formation of a weak wave packet behind the disturbance, which is caused by the destabilizing effect from the long negative tail. Since the wave packet has a lower propagation velocity than the localized disturbance, it disappears outside the figure further downstream. The disturbance amplitude associated with the localized disturbance close to the centreline has a maximum around $x = 300 - 400$ mm, whereafter it starts to decay. Instead, new disturbances appear on both sides of the centreline, and the plot for $x = 500$ mm shows two Λ-shaped structures which resemble the one seen on the centreline in the suction case. However, despite a smaller peak-to-peak amplitude of the localized disturbance, the interaction in the suction case is stronger and generates a larger disturbance amplitude at a specific x-position than in the injection case.

The wall-normal distributions measured on the centreline are shown in figure 14. Since the most interesting events in the case of injection occur aside of the centreline, the plots provide limited information for that case. However, in the suction case it is possible to detect and follow the origin of the strong negative region that evolves on the centreline. At the first x-position (200 mm) one can observe a slightly enhanced wave-trough in the front part of the localized disturbance ($t \approx 42$ ms). If the wave-trough is assumed to propagate with the phase-velocity of the TS-wave ($0.42U_0$), it should be observed at $t \approx 77$ and 113 ms at the following two stations. Apparently there is a local amplification of the TS-wave on the centreline. If the origin of the amplified wave-trough is compared with the plots of the second derivatives of the mean velocity field (figure 10), it is interesting to notice that the amplification starts in the region of the wall-normal inflection point.

4.4. Spectral representation of the interaction

The spanwise distributions in figure 13 were Fourier decomposed, leading to the spectra shown in figure 15. Zero-padding is applied in the spanwise direction in order to keep a constant spatial domain in the Fourier transformation (c.f. discussion in section 2.3). Since the TS-wave has a finite amplitude at the spanwise boundaries of the measured region, a step is introduced when additional zeros are padded. Consequently, artificial 3D components appear in the spectra for $f = 120$ Hz. This artifact is reduced by using a window

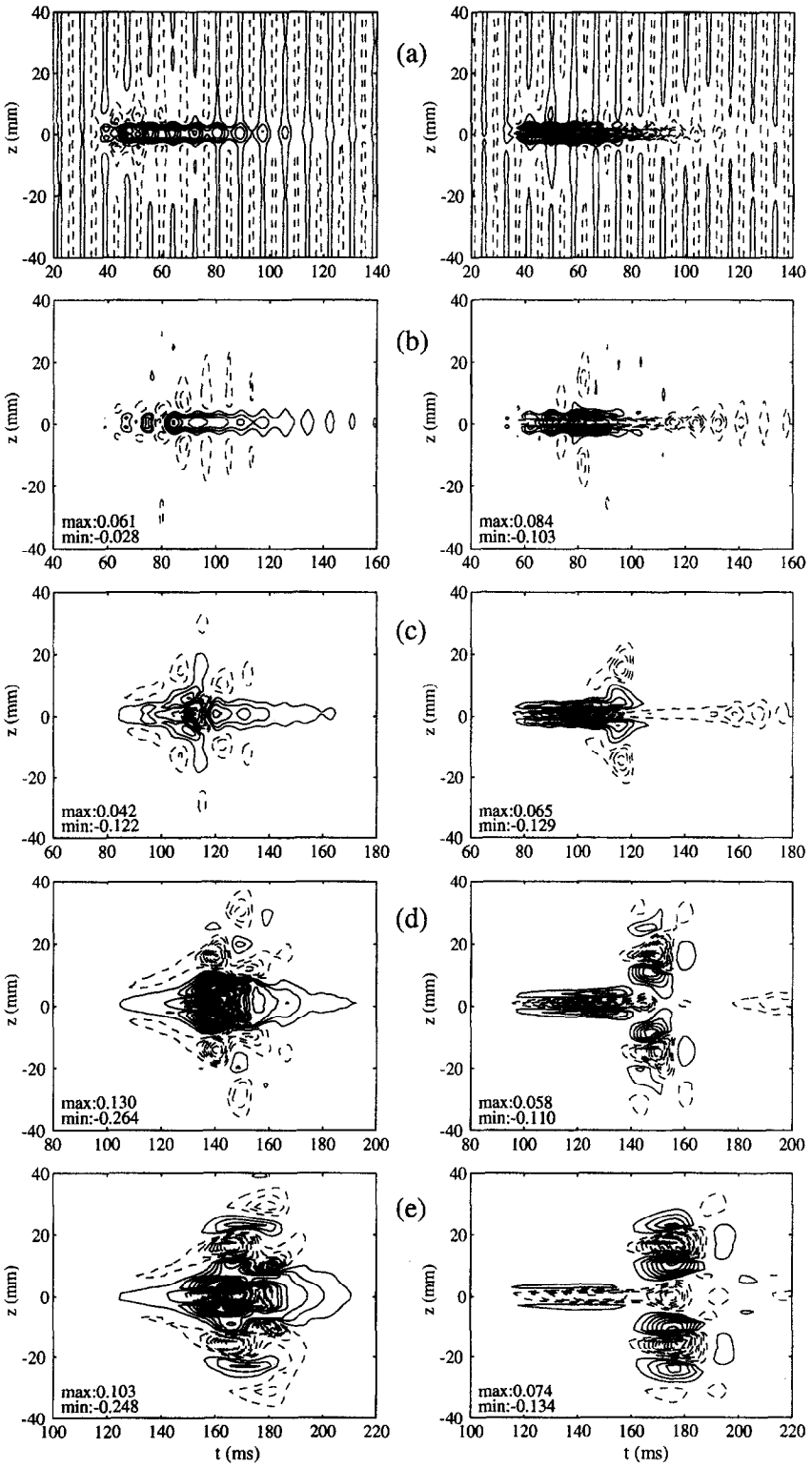

Fig. 13. – Spanwise distributions of the perturbation velocity (u) for the interaction between the localized disturbances and the TS-wave in experiment B. The x-positions are (a) 200 mm, (b) 300 mm, (c) 400 mm, (d) 500 mm and (e) 600 mm. Left and right columns correspond to suction and injection respectively. Contour spacing: $0.01U_0$.

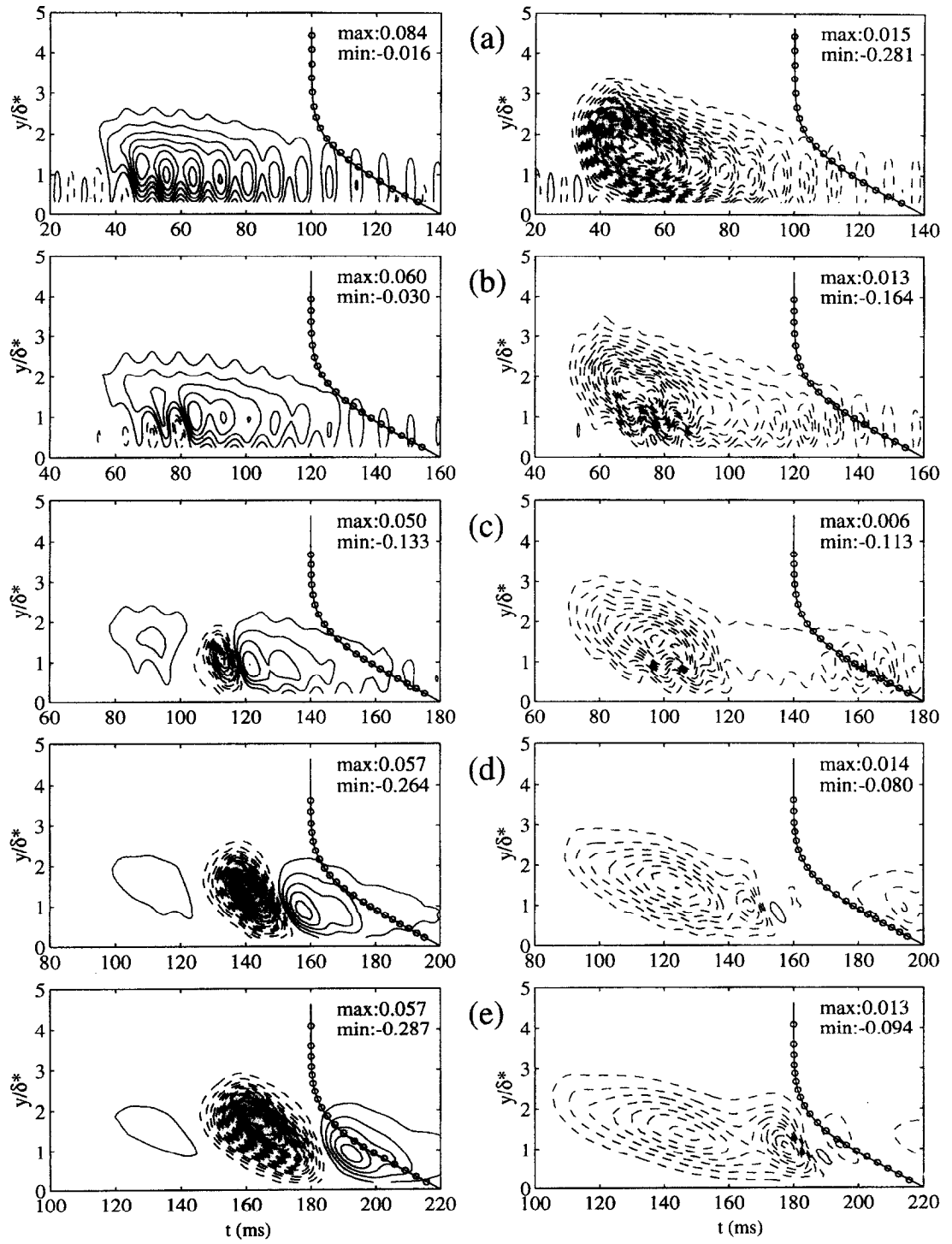

Fig. 14. – Wall-normal distributions measured at $z = 0$ for the interaction between the localized disturbances and the TS-wave in experiment B. The x-positions are from top to bottom 200, 300, 400, 500 and 600 mm. Left and right columns correspond to suction and injection respectively. Contour spacing: $0.01U_0$.

(Kaiser-Bessel) in the spanwise direction for the frequency component of the TS-wave, but still some effect can be observed in the spectra.

The spectra for $x = 200$ mm (not shown) are dominated by the TS-wave and the low-frequency contributions from the localized disturbances. This implies that any contribution from the interaction must be hidden within these spectral components. At the following station, however, energy appear in a wide frequency band (0–120 Hz) and centred at spanwise wavenumbers of $\beta \approx \pm 35$. A similar behaviour can be observed both for the suction and the injection case. Continuing downstream, the same spanwise wavenumbers are increasing in amplitude, but with a concentration of energy in the frequency band 30–40 Hz. Between 400 and 500 mm rather big changes occur, and new dominating spectral peaks appear at $\beta \approx \pm 60 - 70$ m^{-1} and low frequencies. This can be associated with the alignment of the Λ-shaped structures with the flow, resulting in new streamwise streaks. In connection with the results in experiment A, this was explained as a non-linear interaction between the oblique modes (f_1, β_1) leading to transfer of energy to $(0, 2\beta_1)$. The same explanation can be applied to experiment B, in which $f_1 \approx 30 - 40$ Hz, $\beta_1 \approx \pm 30 - 40$ m^{-1}, and the components at $2\beta_1$ are associated with the peaks at $\beta \approx \pm 60 - 70$ m^{-1}. At the last x-position even larger β-components ($\beta = \pm 110 - 130$ m^{-1}) appear in the spectra, centred around the β-axis (i.e. $f = 0$). It should be emphasized that without the forced TS-wave, the qualitative shape of the spectra were similar to those shown in figure 9 for all x-positions (*see* also part 1). This should be compared with the large spectral changes that is observed when the interaction occurs.

Considering the spectral distributions in the two cases (suction and injection), it seems that the scenario is similar, although the amplitudes of the spectral peaks are slightly larger in the case of suction. However, when looking at the distributions of the perturbation velocity in figure 13, relatively large differences are observed. For instance, the positions of the Λ-shaped structures appear at different locations in space, and in the suction case there is a very strong negative peak on the centreline which is absent in the case of injection. Apparently there must be differences which can not be explained by the disturbance spectra. An attempt to decompose the disturbance structure is described in the following section.

4.5. Filtering

In order to relate certain spectral components to different regions in the disturbed flow field, the spectra are filtered and retransformed to physical space. The method is described in figure 16a-d. For the full spectrum (figure 16a), rather distinct bands can be distinguished in the β-direction, and the idea is to filter the spectra according to the bands which are marked in figure 16a. The width of the different bands is determined by the pronounced minima in the spectra. It should be emphasized that all frequencies are maintained within each band, and the spectra is only filtered for different spanwise wavenumbers.

The retransformed signal for the bands B1−, B1+ and their superposition are shown in figures 16b-d. Band B1 has a peak for non-zero frequencies and $\beta \approx \pm 30 - 40$, and the formation of oblique waves becomes evident when plotting the bands individually. Apparently, the major energy contribution is very localized in the streamwise direction, and covers less than one streamwise wave length. The short streamwise extent makes it difficult to accurately determine the frequency, and this might explain why energy is spread over such a wide range of frequencies in the spectra.

Figures 16e and f show the flow fields associated with band B2. This band is dominated by low frequencies, which results in structures more aligned with the flow than in band B1. As mentioned before, band B2 is assumed to be the result of a non-linear interaction between B1− and B1+. It is interesting to look at the phase of the two disturbance fields in figures 16d and f. On the centreline, band B2 counteracts the disturbance due to band B1, while at $z \approx \pm 15$ mm both disturbance fields exhibit negative u. This is equivalent to the positions where the Λ-shaped structures appear.

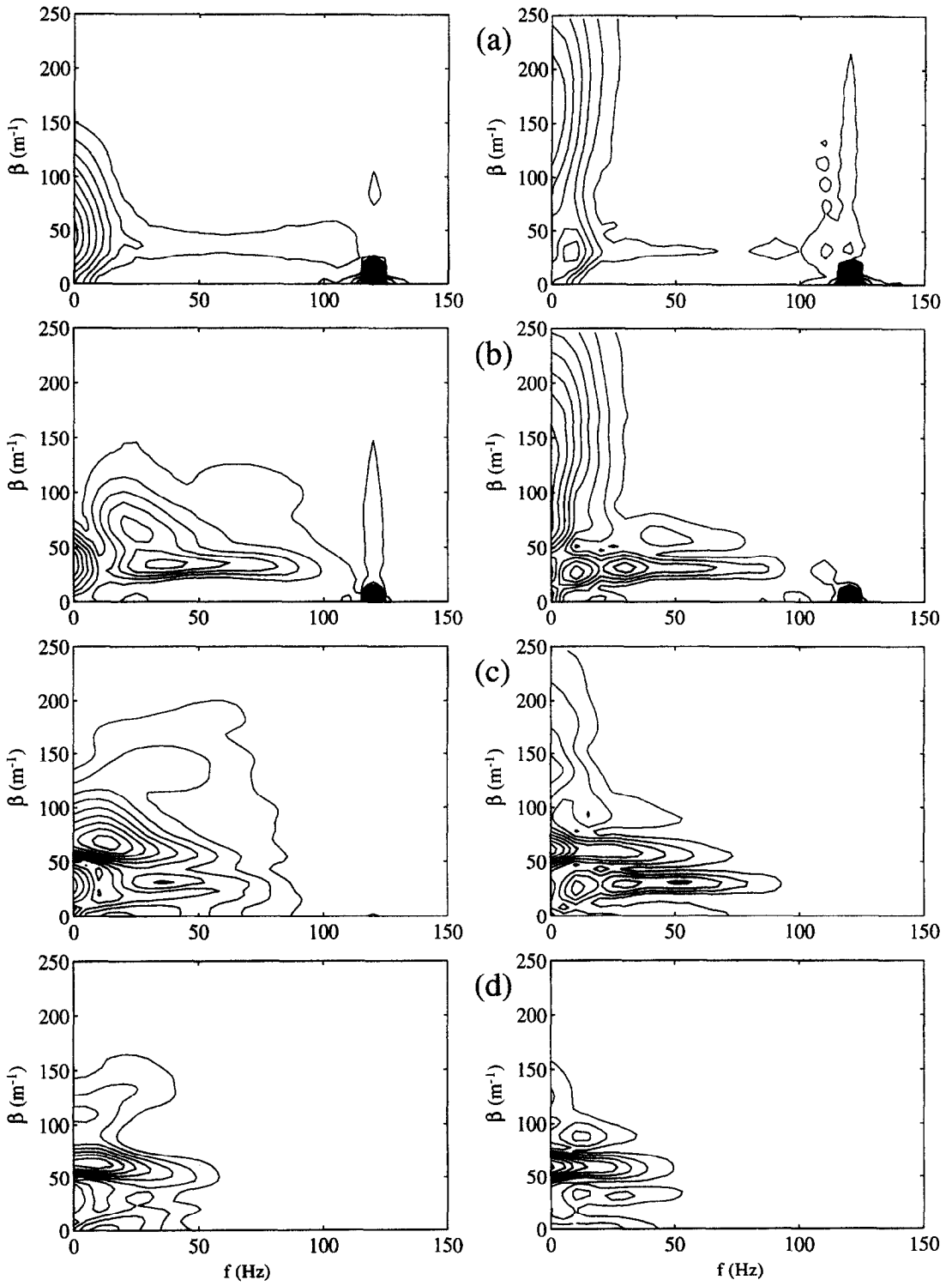

Fig. 15. – Amplitude spectra for the interaction between the localized disturbances and the TS-wave in experiment B. The x-positions are from top to bottom 300, 400, 500 and 600 mm. Contour spacing: (a) 0.005; (b) 0.005; (c) 0.01; (d) 0.02. Left and right columns correspond to suction and injection respectively (only positive β are shown).

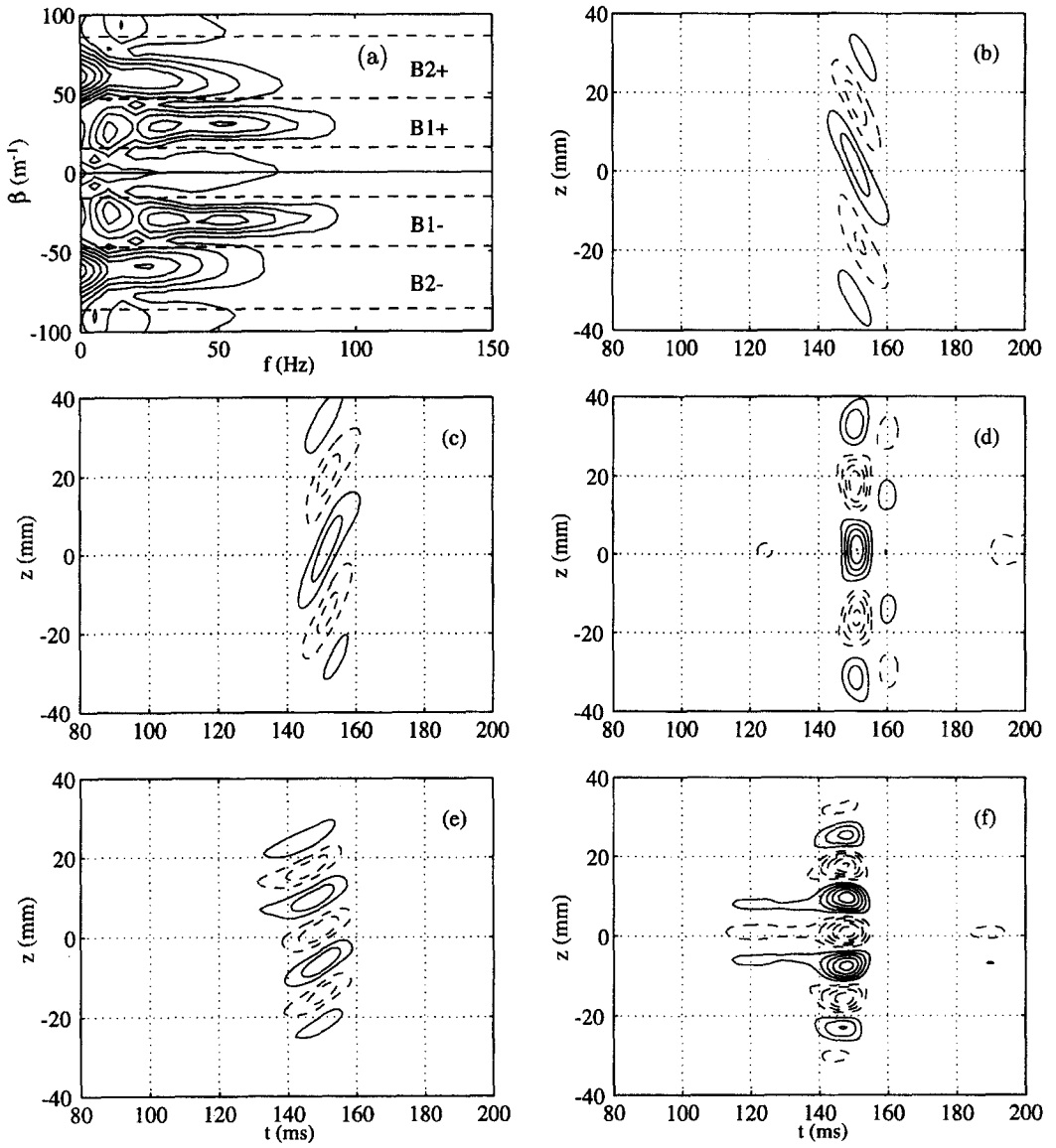

Fig. 16. – (a) (f, β)-spectrum at $x = 500$ mm (injection case) with the different bands defined. The filtered and retransformed flow fields correspond to bands (b) B1−; (c) B1+; (d) B1− & B1+; (e) B2+; (f) B2− & B2+. Contour spacing: $0.01U_0$..

The corresponding filtered flow fields for the suction case are shown in figure 17. The flow field associated with band B1 is similar to the one seen in the injection case, but with opposite phase. If we assume that a non-linear interaction occurs between two oblique modes, the resulting streaks should have an identical spanwise pattern as for the interaction between two waves with a phase shift of π. This is also corroborated in figure 17d, which shows a strong resemblance with figure 16f. This means that the flow fields associated with bands B1 and B2 both have a negative perturbation on the centreline, leading to the strong negative disturbance observed in the suction case.

It should be emphasized that the large difference between the two cases also depends on the short streamwise region of the wave that is amplified. If more than one wave-trough was amplified, the flow field associated with

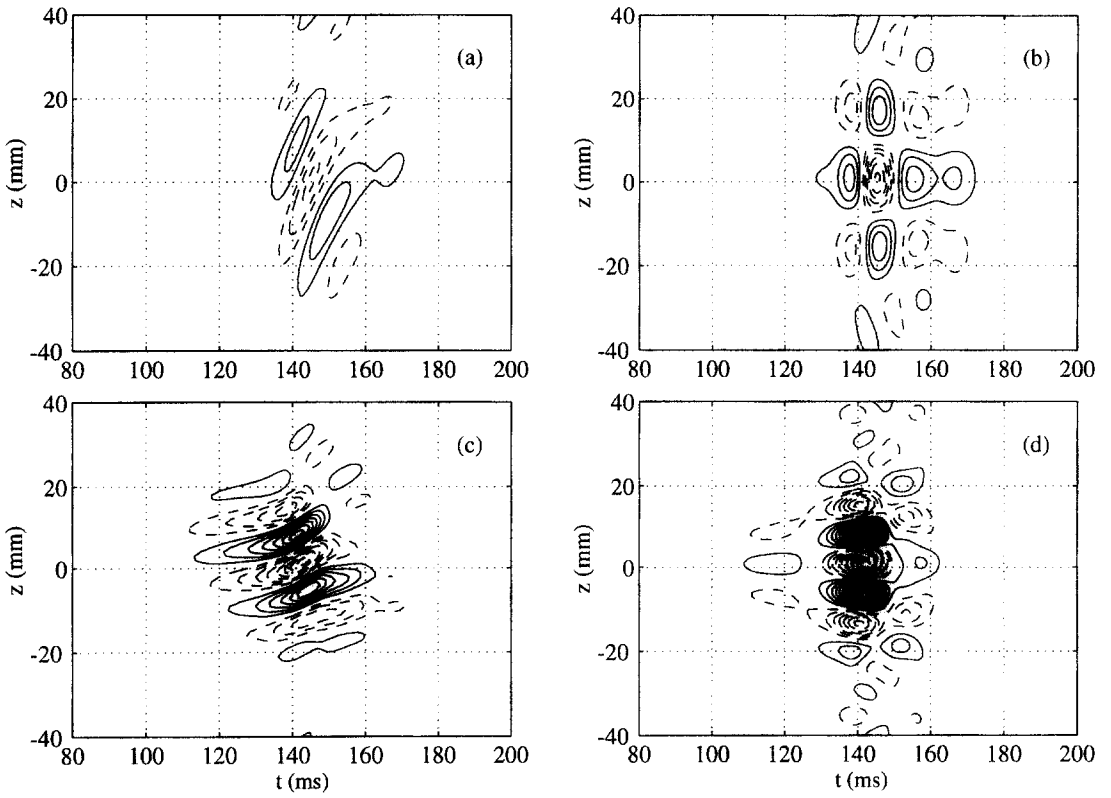

Fig. 17. – Flow fields corresponding to bands
(a) B1+; (b) B1− & B1+; (c) B2+; (d) B2− & B2+; $x = 500$ mm, suction case. Contour spacing: $0.01U_0$.

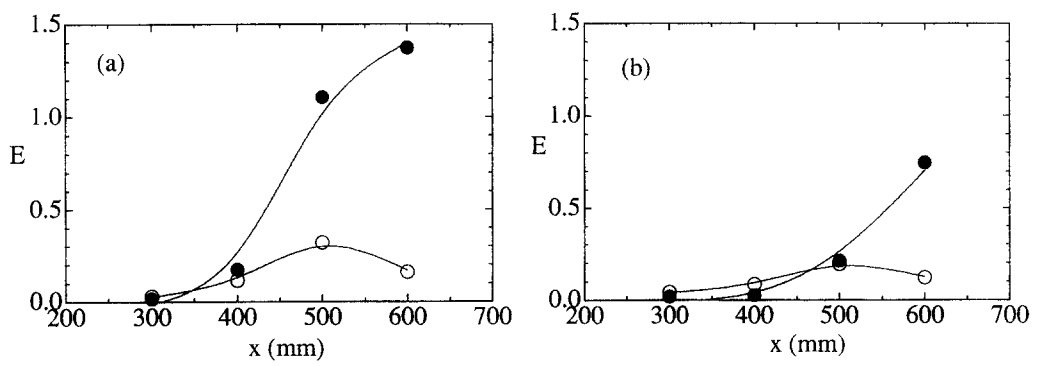

Fig. 18. – Energy in different bands of spanwise wavenumber. Labels: Band B1 (o); B2 (•); curvefit (—). (a) Suction, (b) Injection. ($E = \frac{1}{TZ}\int_0^T \int_{-Z/2}^{Z/2} u^2(t,z)\,dt\,dz$, in which T and Z are the considered time and z-domain respectively).

band B1 should have been periodic in x. In that case a favourable phase relation between B1 and B2 would have been possible on the centreline also in the injection case.

In figure 18 the energy in different bands of spanwise wavenumber is plotted for the two cases. Since the energy is extracted from one spanwise distribution, the plot can only give a qualitative measure of the energy contents. However, at least on the centreline the peaks associated with the interaction have rather wide maxima inside the boundary layer, and the exact y-position for the measured distribution may not be very critical. The

figure shows that the energy in band B1 has a maximum at $x = 500$ mm in both cases, but with a larger magnitude in the suction case. Apparently the localized disturbance in the suction case gives better conditions for the amplification of low-frequency oblique waves than in the case of injection. This might be due to a larger energy content within band B1 in the localized disturbance in the suction case. Moreover, the non-linear generation of energy in band B2 starts earlier in the suction case and results in a stronger growth, although measurements further downstream were not undertaken to detect the subsequent development of the energy in the case of injection.

5. Discussion

Three main stages of the interaction between the TS-waves and the localized disturbances have been revealed in the present paper.

Stage 1: Wave-streak-interaction

A non-linear interaction between a 2D TS-wave with frequency f_0 and a localized disturbance with energy centred around $\pm\beta_0$ and $f = 0$ should, according to the summation of the wave-number vectors in the spectral plane, result in peaks at $(f_0, \pm\beta_0)$. This non-linear interaction was only observed in experiment A, which might be explained by the large initial amplitude of the TS-wave (about 2.5% of U_0 close to the source). In experiment B the initial amplitude of the TS-wave was much smaller, and no evident peaks were found around $(f_0, \pm\beta_0)$.

One fundamental question in the present experiment is why the strongest interaction is observed for high frequencies of the TS-wave? Although no detailed study were undertaken to determine the "optimal frequency", both experiments indicate that the most efficient interaction occur for damped TS-waves. One possible explanation might be the existence of local inflection points in the flow field, since the unstable region for TS-waves is shifted to higher frequencies for inflectional mean velocity profiles. For both suction and injection in experiment B, growing wave packets with a central frequency of 120 Hz were found close to the positions of the inflection points in the instantaneous mean velocity profiles (figure 10). Further downstream the inflectional profiles disappear due to the decreased amplitude of the localized disturbances, leading to decaying wave packets.

While the wave-streak interaction was only observed in experiment A, local inflectional instabilities seemed to be more pronounced in experiment B. Despite these differences, the following stages (2 and 3) were similar in both experiments. This indicates that the first stage of the interaction is not so critical for the final development of the structure.

Stage 2: Formation of oblique structures

The second stage represents a growth of energy at a wide frequency band centred at rather low frequencies, and with a dominant spanwise wave-number (denoted as β_1 in the present paper). In experiment A β_1 is smaller than the dominating wave length in the localized disturbance (β_0), while in the suction case of experiment B β_1 is closer to β_0.

An attempt was done to understand the rapid growth of energy in the oblique modes at stage 2. There are indications that the energy growth is caused by a resonance mechanism comparable to those seen in subharmonic transition. Craik (1971) formulated two necessary conditions for the existence of a three-wave non-linear interaction between a 2D wave and a pair of oblique waves (C-triad). First of all, the frequency of the fundamental (2D) wave should be twice as large as the frequency of the oblique waves, and, secondly, the wavenumber of the fundamental wave should be twice as large as the streamwise wavenumber of the oblique modes. These rather strict requirements have later been relaxed using quasi-steady reasoning (*see* e.g. Kachanov and Levchenko 1984). If the frequency of the subharmonic wave is not exactly half of that of the fundamental

wave, it can still be interpreted as a wave with $f_0/2$ but with a slowly varying phase and amplitude. Kachanov and Levchenko observed amplification in a wide frequency band centred around $f_0/2$, with peaks appearing at $f_0/2+\Delta f$ and $f_0/2-\Delta f$. This is often denoted as *detuned* subharmonic resonance. Weakly non-linear stability theory has confirmed that exact phase synchronization is not a necessary requirement for the amplification of subharmonics (c.f. Zelman and Maslennikova, 1993), and the maximum subharmonic growth is obtained for different wave angles depending on the initial amplitude of the 2D fundamental wave.

In the present experiment the phase was extracted for the available x-positions in experiment B, and there seemed to be a phase coherence between the forced TS-wave and the low-frequency components at $\beta_1 \approx \pm 35$ m^{-1}. The phase coherence was observed in the streamwise region $x \in [300, 500]$ mm. Although the 2D and the 3D waves exhibit roughly the same phase velocities, the second synchronism condition required for a C-triad is not fulfilled. In experiment B the growing oblique components are spread over a wide range of frequencies, but with a dominant peak at 35 Hz. This is not very close to $f_0/2 = 60$ Hz, and there is no corresponding peak at $f_0 + \Delta f = 85$. However, one should bear in mind that the structures corresponding to band B1 in the spectra have a very short streamwise extent, and contain barely one period of the wave. Accordingly, one should not be surprised that energy is spread over a wide range of frequencies, without a well defined peak. Since only one wave-trough is strongly amplified on the centreline in the suction case, with a significant downstream dispersion as well, it seems plausible that a propagation velocity in agreement with the forced TS-wave should be a sufficient condition for resonance in the present situation.

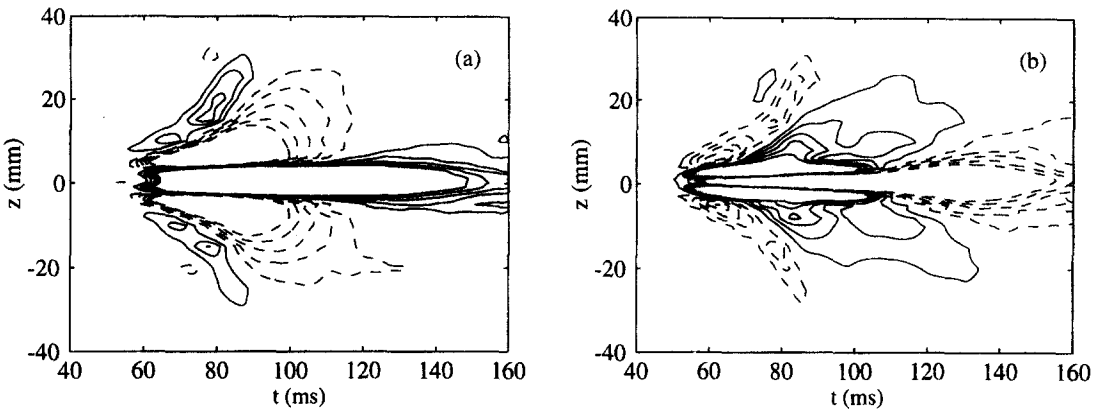

Fig. 19. – Spanwise distribution of the localized disturbances at $x = 300$ mm.
Contours are plotted from $-0.005U_0$ to $+0.005U_0$ with spacing $0.001U_0$. (a) Suction; (b) Injection.

The fact that amplification is observed only for one period of the wave deserves further attention. The amplified region originates from the front part of the localized disturbance, which coincides with the local inflection points caused by the presence of the localized disturbance. However, another possible explanation for the local amplification can be found in figure 19. The disturbance field due to the localized disturbance is plotted with a finer contour spacing (0.1% of U_0), which in the suction case reveals a wedge shaped wave-crest emanating from the leading edge of the localized disturbance. The injection case exhibits, at least qualitatively, a similar wave but with opposite phase. It is possible that these three-dimensional waves interact with the TS-wave, resulting in a local resonance phenomenon.

Stage 3: Formation of streaky structures

The last stage in the interaction process is also the one which can be best understood based on earlier experimental and numerical studies, and it shows similarities with the mechanisms that are often denoted as

oblique transition. Two oblique waves that interact non-linearly result in streamwise vortices, which in turn generate strong low- and high-velocity streaks in the u-component (*see* e.g. Berlin *et al.* 1994). The spanwise wavenumber of the streaks should be twice as large as β of the forcing oblique wave. Both in experiment A and B energy was shifted to frequencies close to zero and $\beta \approx 2\beta_1$ (β_1 was approximately ± 65 m^{-1} in experiment A and $\pm 30 - 40$ m^{-1} in experiment B). The non-zero frequency is due to the small spatial extent of the generated streaks, and other disturbances can together with the streaks form a streamwise periodicity, which will result in a non-zero central frequency in the spectra.

The later stages of the development of the present disturbance can be compared with observations made by Gaster and Grant (1995) and by Breuer *et al.* (1997) on the breakdown of a wave packet. Breuer *et al.* (1997) introduced a weak localized disturbance in the boundary layer at supercritical Reynolds numbers, resulting in a growing wave packet dominated by 2D and 3D TS-waves. The non-linearity starts with growing oblique subharmonic modes, followed by a so-called beta-cascade: if f_1 and β_1 indicate frequency and spanwise wavenumber for the subharmonic modes, non-linear interactions will transfer energy to $(0, 2\beta_1)$, $(f_1, 3\beta_1)$ etc. The velocity field for the wave packet deforms during this development first into an arrow shaped structure, followed by an increasingly streaky structure. Breuer *et al.* point out the strong resemblance between the structure seen in their experiment, and a simulation by Breuer and Landahl (1990), in which a strong localized disturbance was introduced at a supercritical Reynolds number R. Also in the experiment by Shaikh and Gaster (1995), using white noise excitation, a Λ-shaped structure appeared prior to the formation of a turbulent spot. It should be emphasized that there are large differences in initial conditions between the different studies. In the experiments of Breuer *et al.* and the calculations by Breuer and Landahl the energy in three dimensional modes was either introduced through a strong initial disturbance or a wave packet passing through the linear and non-linear regimes. Shaikh and Gaster obtained strong non-linear events from small amplitude TS-waves excited by white noise generated from a loud speaker in the plate. The Reynolds numbers were in all three cases rather high. In the present experiment the energy in three dimensional modes appeared due to a non-linear interaction at low Reynolds numbers.

6. Conclusions

The observations from the present measurements can be summarized as follows:

(i) Strong interaction between a localized disturbance and a damped high-frequency TS-wave has been observed at low Reynolds numbers. The interaction starts in the front part of the localized disturbance, and the amplified part of the wave includes barely one streamwise wavelength of the TS-wave.

(ii) A major stage in the downstream development is the formation of oblique structures, associated with a wide band of low-frequency components in the spectra (B1). These oblique waves exhibit a spanwise spreading during the downstream development. Subharmonic resonance was found to play an essential role in the observed interaction at this stage.

(iii) Once a strong oblique structure has formed, energy is non-linearly transferred to spectral peaks with frequencies close to zero and twice as large spanwise wavenumber (B2) as the oblique structure. This corresponds to the formation of new streamwise streaks, which is comparable with observations made at transition caused by a pair of oblique waves.

(iv) Due to the phase relation between the flow fields associated with band B1 and B2, a strong negative disturbance is observed on the centreline in the case of suction. In the injection case the corresponding flow fields counteract each other on the centreline, while further downstream strong disturbances appear on either side of the localized disturbance.

Berlin *et al.* (1994), conjectured a universal breakdown process when starting from oblique waves in shear flows. Two oblique waves that interact non-linearly result in streamwise vortices, which in turn generates powerful low- and high-velocity streaks in the u-component. This is usually denoted as *lift-up* (*see* also part 1) after ideas by Landahl (1977, 1980). The formation of streaks from two oblique waves has also been verified experimentally in the case of plane Poiseuille flow (Elofsson and Alfredsson, 1995), as well as in Blasius flow (Wiegel 1996, Elofsson and Alfredsson 1997). Furthermore, it is suggested that the final breakdown into turbulence is initiated by secondary instabilities of the streaks, which appear when they exceed some threshold amplitude. This was initially observed as non-stationary motions of the streaks in the simulation of Berlin *et al.*, and similar observations have also been made in Direct Numerical Simulations of plane Poiseuille flow and plane Couette flow (*see* Henningson 1997 for a summary).

In the present experiment the simultaneous generation of a localized streaky structure and periodic TS-waves did not result in motions which can be associated with secondary instabilities of the streaks, and the strong spanwise gradients in the injection case did not cause any observable instability. Probably the absence of secondary instabilities can be ascribed to the perturbation amplitude, which might be too small for the relatively low Reynolds numbers that are considered in the present study. Recent experiments at the Royal Institute of Technology on secondary instabilities of longitudinal streaks in boundary layers as well as Poiseuille flow indicate that large spanwise gradients are required to observe natural secondary instabilities (Kawakami *et al.* 1997). Instead of secondary instabilities, an interaction between the localized disturbance and the TS-wave was observed in the present experiment, leading to growth of energy at low frequencies and non-zero spanwise wavenumbers.

In the study by Boiko *et al.* (1994) it was shown that the generation of TS-waves in a boundary layer subjected to FST resulted in energy growth at low frequencies. Moreover, spanwise correlation measurements at the TS-wave frequency showed a reduced correlation when the FST-level was high. A plausible interpretation is that the streaky structures break the initial two-dimensionality of the wave fronts, thus promoting the formation of 3D-structures. Since the streaks in a boundary layer subjected to FST appear irregularly in time and space, local interactions similar to the one studied in the present paper may well be of importance. Since FST also can excite TS-wave packets with larger growth rates than predicted by linear theory (Kendall 1993), local three dimensional TS-waves can be involved in similar interactions with the streaks. Hence, interaction between localized streaky structures and TS-waves might be a candidate for the breakdown of a boundary layer subjected to moderate levels of FST.

Acknowledgements. – This work was supported by the Swedish National Board for Industrial and Technical Development (NUTEK), and the position at KTH of Dr. A.A. Bakchinov was sponsored by the Göran Gustafsson Foundation and the Swedish Institute (SI). The visits to KTH of Prof. V.V. Kozlov and Dr. A.A. Bakchinov were supported by the Royal Swedish Academy of Sciences (KVA) and the Göran Gustafsson Foundation. We wish to thank A. Hanifi for the PSE-calculations, and P. Elofsson for providing us with the equipment for the TS-wave generation.

REFERENCES

BAKCHINOV A. A., GREK G. R., KLINGMANN B. G. B., KOZLOV V. V., 1995a, Transition experiments in a boundary layer with embedded streamwise vortices, *Phys. Fluids*, **7** (4), 1820–832.

BAKCHINOV A. A., WESTIN K. J. A., KOZLOV V. V., ALFREDSSON P. H., 1995b, On the receptivity of a flat plate boundary layer to localized free stream disturbances. In *Laminar-Turbulent Transition*, KOBAYASHI R. Ed., Springer-Verlag, 341–348.

BAKCHINOV A. A., GREK G. R., KATASONOV M. M., KOZLOV V. V., 1997, Experimental study of localized disturbances and their development in a flat plate boundary layer, Preprint No. 1-97, ITAM, Russian Academy of Sciences, Novosibirsk (in Russian).

BAKE V., KACHANOV Y. S., FERNHOLZ H. H., 1995, Subharmonic K-regime of boundary-layer breakdown. In *Proc. Colloquium on Transitional Boundary Layers in Aeronautics,* HENKES R. A. W. M., VAN INGEN J. L., Eds., Amsterdam: December 6-8, 1995, pp.81-88.

BERLIN S., LUNDBLADH A., HENNINGSON D. S., 1994, Spatial simulations of oblique transition in a boundary layer, *Phys. Fluids*, **6**, 1949–1951.

BOIKO A. V., WESTIN K. J. A., KLINGMANN B. G. B., KOZLOV V. V., ALFREDSSON P. H., 1994, Experiments in a boundary layer subjected to free stream turbulence. Part 2. The role of TS-waves in the transition process, *J. Fluid Mech.*, **281**, 219–245.

BOTTARO A., KLINGMANN B. G. B., 1996, On the linear breakdown of Görtler vortices, *Eur. J. Mech., B/Fluids*, **15**, 301–330.

BREUER K. S., COHEN J., HARITONIDIS J. H., 1997, The late stages of transition induced by a low-amplitude wave packet in a laminar boundary layer, *J. Fluid Mech.*, **340**, 395–411.

BREUER K. S., LANDAHL M. T., 1990, The evolution of a localized disturbance in a laminar boundary layer. Part II: Strong disturbances, *J. Fluid Mech.*, **220**, 595–621.

CRAIK A. D. D., 1971, Nonlinear resonant instability in boundary layers, *J. Fluid Mech.*, **50**, 393–413.

ELOFSSON P. A., ALFREDSSON P. H., 1995, Experiments on nonlinear interaction between oblique Tollmien-Schlichting waves. In *Laminar-Turbulent Transition*, Kobayashi R. Ed., Springer-Verlag, 465–472.

ELOFSSON P. A., ALFREDSSON P. H., 1997, An experimental investigation of oblique transition in a Blasius boundary layer, EUROMECH Colloquium 359, Stuttgart.

GAPONENKO V. R., KACHANOV Y. S., 1994, New methods of generation of controlled spectrum instability waves in the boundary layer. In *Proc. International Conference on Methods of Aerophysical Research*, Novosibirsk: Inst. Theor. & Appl. Mech., Part **1**, 90–97.

GASTER M., GRANT I., 1975, An experimental investigation of the formation and development of a wave packet in a laminar boundary layer, *Proc. Roy. Soc. Lond. Ser. A*, **347**, 253–269.

GREK H. R., DEY J., KOZLOV V. V., RAMAZANOV M. P., TUCHTO O. N., 1991, Experimental analysis of the process of the formation of turbulence in the boundary layer at higher degree of turbulence of windstream, Technical Report 91-FM-2, Indian Inst. Science, Bangalore, 560012, India.

GREK H. R., KOZLOV V. V., RAMAZANOV M. P., 1987, Laminar-turbulent transition in the presence of a high level of free stream turbulence, *Izv. Akad. Nauk SSSR, Mekh. Zhid. Gaza.* **6**, 34–41. (in Russian, English transl. 1988 in *Fluid Dyn.* **23**:6, 829–834).

GREK H. R., KOZLOV V. V., RAMAZANOV M. P., 1990, Receptivity and stability of the boundary layer at a high turbulence level. In *Laminar-Turbulent Transition*, Arnal D., Michel R. Eds., Springer-Verlag, 511–521.

HENNINGSON D. S., 1995, Bypass transition and linear growth mechanisms. In *Advances in Turbulence V*, Benzi R. Ed., Kluwer, 190–204.

KACHANOV Y. S., LEVCHENKO V. Y., 1984, The resonant interaction of disturbances at laminar turbulent transition in a boundary layer, *J. Fluid Mech.*, **138**, 209–247.

KACHANOV Y. S., TARARYKIN O. I., 1987, Experimental study of stability of a relaxing boundary layer. *Izv. Sib. Otd. Akad. Nauk SSSR, Ser. Tekh. Nauk*, **18** (5), 9–19 (in Russian), (see also *Separated flows and jets*, 1991, Kozlov V. V., Dovgal A. V. Eds., Springer, 737–740).

KAWAKAMI M., ELOFSSON P., ALFREDSSON P., 1997, Experiments on the stability of streamwise streaks in plane Poiseuille flow. Technical Report TRITA-MEK 1997:16, Dept. of Mechanics, Royal Institute of Technology, Stockholm.

KENDALL J. M., 1993, Boundary layer receptivity to weak freestream turbulence, Notes on figures presented at End-Stage Transition Workshop, August 15, 1993.

KLINGMANN B. G. B., Boiko A. V., WESTIN K. J. A., KOZLOV V. V., ALFREDSSON P. H., 1993, Experiments on the stability of Tollmien-Schlichting waves, *Eur. J. Mech., B/Fluids*, **12**, 493–514.

LANDAHL M. T., 1977, Dynamics of boundary layer turbulence and the mechanism of drag reduction, *Phys. Fluids*, **20**, (10, Part II), 55–63.

LANDAHL M. T., 1980, A note on an algebraic instability of inviscid parallel shear flows, *J. Fluid Mech.*, **98**, 243–251.

MALIK M. R., HUSSAINI M. Y., 1990, Numerical simulation of interactions between Görtler vortices and Tollmien-Schlichting waves, *J. Fluid Mech.*, **210**, 183–199.

MEITZ H., 1996, *Numerical investigation of suction in a transitional flat-plate boundary layer.* PhD thesis, The University of Arizona, Department of Aerospace and Mechanical Engineering, Tucson, AZ.

SHAIKH F. N., GASTER M., 1995, The natural evolution of turbulent spots in a flat plate laminar boundary layer. In *Laminar-Turbulent Transition*, Kobayashi R. Ed., Springer-Verlag, 271–278.

WESTIN K. J. A., BOIKO A. V., KLINGMANN B. G. B., KOZLOV V. V., ALFREDSSON P. H., 1994, Experiments in a boundary layer subjected to free-stream turbulence. Part I. Boundary layer structure and receptivity, *J. Fluid Mech.*, **281**, 193–218.

WESTIN K. J. A., BAKCHINOV A. A., KOZLOV V. V., ALFREDSSON P. H., 1998, Experiments on localized disturbances in a flat plate boundary layer. Part 1. The receptivity and evolution of a localized free stream disturbance, *Eur. J. Mech., B/Fluids*, **17**, (6) 823–846.

WIEGEL M., 1996, *Experimentelle Untersuchung von kontrolliert angeregten dreidimensionalen Wellen in einer Blasius-Grenzschicht.* PhD thesis, TH Hannover.

ZELMAN M. B., MASLENNIKOVA I. I., 1993, Tollmien-Schlichting-wave resonant mechanism for subharmonic-type transition, *J. Fluid Mech.*, **252**, 449–478.

(Manuscript received September 30, 1997,
Revised February 12, 1998;accepted March 12, 1998.)